1. Introduction

Nitrophenanthrene (Nph) derivatives were synthesized by Fukuhara et al. [1,2], and their mutagenicity was investigated in *Salmonella* strains [3]. It was found that most nitro derivatives showed strong mutagenicity in *Salmonella* mutants, and that the orientation of the nitro substituent had an important structural feature affecting the mutagenic potency and metabolism of Nph [3–5]. Normally, mutagenic activity of nitroarenes is associated with structural features such as the physical dimensions of the aromatic rings, isomeric position of the nitro group, conformation of the nitro group with respect to the plane of the aromatic rings and the ability to resonance-stabilize the ultimate electrophile [6].

Aristolochic acid was used as an anti-inflammatory agent in several pharmaceutical preparations up to 1982, and consisted of several components of Nphs [7]. It was found that Aristolochic acid also contained genotoxic mutagens forming DNA adducts after metabolic activation in *Salmonella* strains and mammalian cells [8–10], as well as being was carcinogenic in rats [11–13]. It has been reported that the mutagenic activity of Nph was closely associated with reduction potentials and the dihedral angles of the nitro substituent for intercalation of chemicals into DNA [2–4,14,15].

Nitroazaphenanthrene (NAph) derivatives containing nitrogen atoms at the 1, 4, and 9 positions of phenanthrene rings were synthesized by Fukuhara et al. (unpublished data), and their reduction property was determined. Using authentic samples of Nph and NAph derivatives, *Salmonella* mutagenicity was determined, and the structural activity relationship was discussed.

2. Materials and methods

2.1. Chemicals

NAphs containing nitrogen atoms in the rings used in this study were 8-nitro-1-azaphenanthrene (8-N-1-Aph), 6- and 8-N-4-APh, 4-, 5-, 6-, and 7-N-9-Aph, 5-, 6- and 8-N-1-Aph *N*-oxide (5-, 6- and 8-N-1-AphO), 5-, 6- and 8-N-4-APhO, 1-, 2-, 3- and 5-N-9-APhO, and 1,5- and 1,8-dinitro-4-APhO (1,5- and 1,8-diN-4-AphO). These NAph derivatives were synthesized by Fukuhara et al. (unpublished data) and modified by the method described by Dewar and Warford [16].

2.2. Bacterial strains

Bacterial strains used were *Salmonella typhimurium* TA98, TA100, and TA98NR, a nitroreductase-deficient mutant of TA98, TA98/1,8DNP, an *O*-acetyltransferase-deficient mutant of TA98, YG1021 and YG1026 produced by transferring a plasmid carrying the nitroreductase gene into cells of TA98 and TA100, respectively, and strains YG1024 and 1029, carrying a plasmid of the acetyltransferase gene transferred into cells of TA98 and TA100, respectively, were generously donated by Drs T. Nohmi and M. Watanabe, National Institute of Health Sciences [17].

2.3. Electrochemical reduction by cyclic voltammetry and electronic descriptors

In dimethylformamide, teraethylammonium perchlorate was used as the supporting electrolyte at a 0.1 M concetration. The reference electrode was an Ag/Ag^+ electrode in acetonitrile with 0.1 M tetrabutylammonium perchlorate. After transfer of the solution containing the test chemical to the cell, it was purged of oxygen by bubbling with N_2 for 15 min. The cyclic voltammograms were recorded at a scan rate of 100 mV/s, while maintaining the test solution under a steady steam of N_2.

The electronic descriptor, LUMO energy levels of nitrated phenanthrenes, was calculated by MOPAC2002 (AM1), which is based on the MOPAC of the Toray System Center using the AM1 method. The initial geometries were constructed from standard bond lengths and angles. The geometries were then completely optimized using algorithms in the MOPAC program. For 5-N-4-AphO and 1,5-diN-4-AphO, LUMO energy and dihedral angle were obtained by AM1 calculations based on the structure that was optimized by PM3.

2.4. Mutagenicity test

Mutagenicity was determined by the plate incorporation test using *Salmonella* tester strains [3]. Each experiment was carried out on triplicate plates two times with or without the S9 mix, and the mean value was presented as revertants/μg of chemical.

3. Results

3.1. LUMO energy levels and dihedral angles of Nphs

To measure enzymatic reduction, the LUMO energy levels, reduction potential, and orientation of the nitro substituent to the phenanthrene rings were investigated (Table 1). Nitro substituents substituted at the 4 and 5 positions were perpendicular due to the steric effect of the bay region aromatic proton, while those at the 2, 3, 6, and 7 positions were coplanar to the phenanthrene rings (Fig. 1). In contrast, nitro substituents at the 1 and 8 positions had a nitro function with nearly perpendicular orientation to the aromatic ring system because of steric hindrance of the aromatic proton on the peri position, while the calculated dihedral angles varied between 26° and 33°. This suggested that the orientation of the nitro group generally predicts the mutagenic potency of NAphs. There was no relationship between mutagenicity, reduction potentials and LUMO energy.

Table 1
LUMO energy levels, reduction potentials, and dihedral angles of NAphs

Chemical	Epc (mV)		LUMO	Dihedral angle
	Epc1	Epc2		
8-N-1-Aph	1042	1631	1429	31.5
6-N-4-Aph	1036	1675	1400	0.1
8-N-4-Aph	1058	1555	1372	32.2
4-N-9-Aph	1120	1662	1326	62.6
5-N-9-Aph	1085	1615	1219	61.7
6-N-9-Aph	1027	1645	1508	0.2
7-N-9-Aph	1004	1664	1436	0.0
5-N-1-APhO	1049	1625	1505	61.0
6-N-1-AphO	972	1572	1663	0.1
8-N-1-AphO	988	1641	1623	33.3
5-N-4-APhO	1214	1619	1427	32.2[a]
6-N-4-APhO	1059	1723	1583	0.7
8-N-4-APhO	1047	1678	1545	31.7
1-N-9-APhO	853	1484	1674	26.5
2-N-9-APhO	964	1628	1696	0.1
3-N-9-APhO	893	1463	1733	0.1
5-N-9-APhO	1029	1568	1494	60.3
1,5-diN-4-APhO	623	1263	2074	30.1[b]
1,8-diN-4-APhO	916	1032	2214	58.2*

[a] and [b], LUMO energy and dihedral angle were obtained by AM1 calculations based on the structure that was optimized by PM3.

* 8-NO_2, 33.5; 1-NO_2, 24.7.

3.2. Chemical properties of Nph

Fig. 1 illustrates chemical structures, consisting of Aph derivatives with a nitrogen atom at the 1, 4, and 9 positions, and NAphs, nitrated derivatives, substituted at the 1, 2, 3, 4, 5, 6, 7, and 8 positions in phenanthrene rings and their *N*-oxides.

3.3. Mutagenicity of NAph in Salmonella strains

All NAphs substituted at the 4, 6, 7, and 8 positions were mutagenic for strains TA98 and TA100 without S9 mix while 5-N-9-Aph, 5-N-1-AphO, and 5-N-9-AphO were non-mutagenic or weak mutagens. In NAphO derivatives, 6-N-1-AphO, 8-N-1-AphO, 6-N-4-AphO, and 1, 2, and 3-N-9-AphOs were mutagenic for strains TA98 and TA100, and were direct-acting mutagens, showing activity in the absence of S9 mix while 5-N-1- and 5-N-9-AphOs were non-mutagenic or weakly mutagenic (Table 2). In contrast, mutagenicity for TA98 with S9 mix was assessed, but it was not shown in any NAph derivatives (Table 2). Thus, a mutagenicity test was carried out in the absence of the S9 mix. In these nitrated derivatives, nitro derivatives substituted at the 6 position of phenanthrene rings, 6-N-4-Aph, 6-N-9-Aph, 6-N-1-AphO, and 6-N-4-AphO, showed powerful mutagenicity for strains TA98, TA100, and all YG strains used. Mutagenicity was enhanced by mutant strains producing nitroreductase such as YG1021 and 1026, and those producing *O*-acetyl-

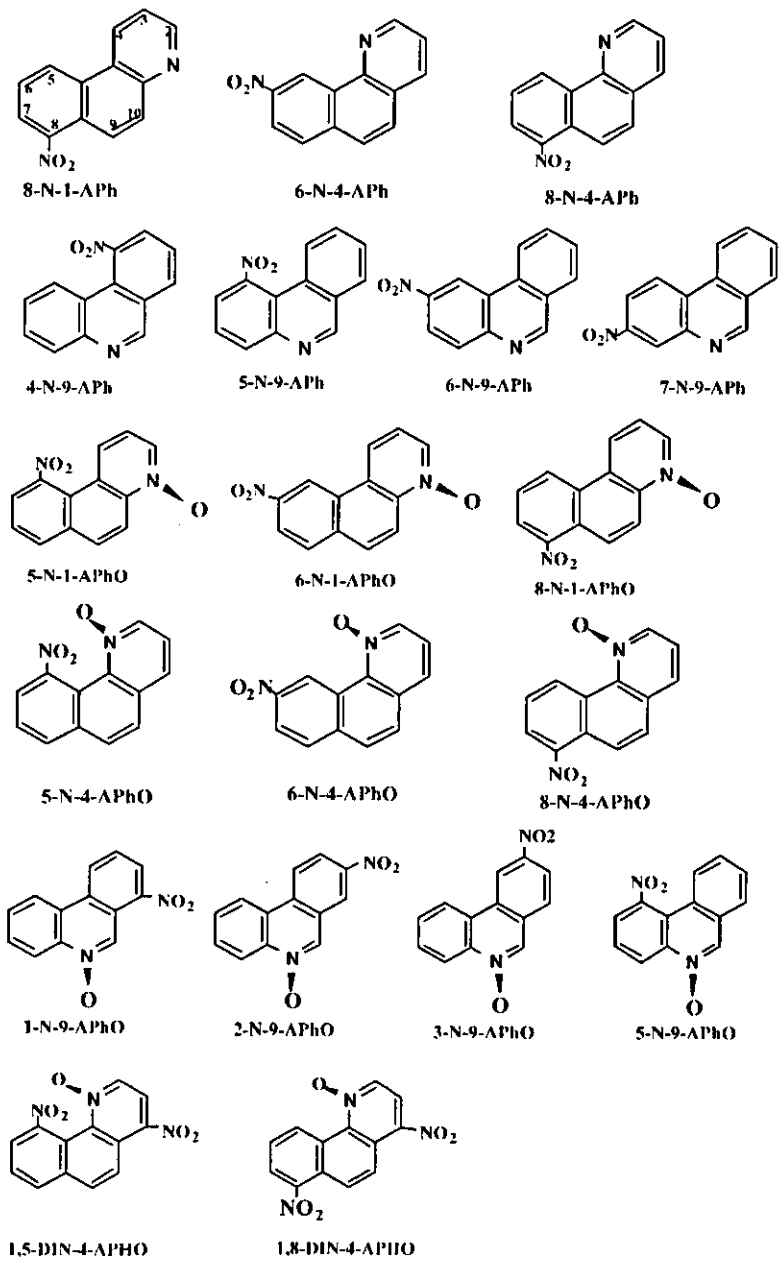

Fig. 1. Chemical structures of NAph's.

transferase such as YG1024 and YG1029. In addition, the nitroreductase activity was also confirmed by the fact that the activity was inhibited by the nitroreductase-deficient strain TA98NR, and similarly, was inhibited by the TA98/1,8-DNP_6. *O*-acetyltransferase-deficient strain. Nitro derivatives substituted at the 8 position of the phenanthrene rings such as 8-N-1- and 8-N-4-Aphs, were strongly reverted from autotrophy to prototrophy for strain TA100. These derivatives might arise due to base pair substitution on DNA, showing higher mutageni-

Table 2
Mutagenicity of Naphs

Chemical	Mutagenicity (revertants/μg)								
	TA98 (−S9)	TA98 (+S9)	TA98NR	TA98/1,8DNP$_6$	TA100	YG1021	YG1024	YG1026	YG1029
Spontaneous	29	28	37	11	128	67	86	178	183
8-N-1-Aph	538	8	42	0.3	1046	8479	35600	13040	1246
6-N-4-Aph	2052	18	149	530	6060	42370	6260	46800	11020
8-N-4-Aph	828		16	141	1528	14480	7980	1282	4018
4-N-9-Aph	112	11	31	48	160	806	609	785	401
5-N-9-Aph	6	ND	2	1.6	7	47	18	53	9
6-N-9-Aph	728	13	168	98	818	1050	3478	5194	788
7-N-9-Aph	452	20	61	185	251	850	1018	918	408
5-N-1-AphO	3	ND	1	0.7	6	16	9	16	8
6-N-1-AphO	150	8	99	82	493	1247	170	5949	718
8-N-1-AphO	38	ND	3	17	113	998	79	1310	122
5-N-4-AphO	63	6	15	19	146	247	87	97	92
6-N-4-AphO	700	17	142	215	1854	6893	1818	7258	4354
8-N-4-AphO	67	ND	4	23	151	1038	786	1528	704
1-N-9-AphO	764	26	170	482	1252	1756	915	4627	897
2-N-9-AphO	213	20	20	36	148	174	639	737	106
3-N-9-AphO	634	11	141	684	173	596	3482	748	413
5-N-9-AphO	4	ND	1	0.5	5	16	12	38	7
1,5-diN-4-AphO	10460	33	6420	1440	2906	24980	11637	9541	6575
1,8-diN-4-AphO	5580	24	5240	8440	8440	21640	11002	48850	5916

ND, not detected.

city in TA100 than TA98. These nitro groups could also be due to steric hindrance of the nitro substituent on the plane of the phenanthrene rings.

Two 1,5- and 1,8-diN-4-AphOs promoted marked mutagenicity for TA98, TA100, and YG strains. Mutagenicity of 1,5- and 1,8-diN-4-AphO corresponded to 166 and 83 times, respectively, that of 5-N-4-AphO and 8-N-4-AphO for TA98, and to 19 and 55 times, respectively, that of 5-N-4- and 8-N-4-AphOs for TA100. Dinitro derivatives substituted at the 1 and 5 positions of the phenanthrene rings were strongly activated by nitroreductase, overproducing mutants more than *O*-acetyltransferase (Table 2). Both dinitro derivatives, which have relatively lower LUMO energy, showed high mutagenicity for strains TA98 and TA100, and their enzyme rich-mutants. It was found that mutagenicity of 1,5- and 1,8-diN-4-AphO was strongly activated by nitroreductase, rather than *O*-acetyltransferase, as shown in YG1021 and 1024, except for reversion for YG 1026 of 1,8-diN-4-AphO.

4. Discussion

We previously reported that the mutagenic potency of Nphs was closely associated with the chemical properties and orientation of nitro substitution of aromatic rings [3]. Nitro substituents at positions 4 and 5 in the phenanthrene rings were perpendicular, while those on positions 2, 3, 6 and 7 were nearly coplanar to the phenanthrene rings (Table 1). It has also been reported that Nphs on positions 1, 8, 9, and 10 were non-coplanar because of steric hindrance of the aromatic proton on the peri position, with dihedral angles varying from 10° to 65° [1,2].

In this study, it was found that NAphs with a nitrogen atom at the 1, 4, and 9 positions of

phenanthrene rings showed potent mutagenicity corresponding to Nphs if they had the same chemical properties as Nphs. Mutagenicity of 4-, 6-, and 7-N-9-Aphs, 1-, 2-, and 3-N-9-AphOs, was potent for *Salmonella* strains, while nitro substituents of 5-N-9-Aph, 5-N-1-AphO, and 5-N-9-AphO were non- or weakly mutagenic. The nitro substituent at the 5 position in the rings was perpendicular on the plane of phenanthrene rings, so mutagenicity was reduced markedly due to steric hindrance. This suggested that the mutagenic potency of these nitro groups closely involved the orientation of nitro substituents of the phenanthrene rings, and the inability to intercalate into the DNA helix.

Nitro substituents on positions 2, 3, 6, and 7 in the phenanthrene rings had a nitro function with coplanar orientation to the parent rings, and had relatively lower LUMO energy levels. In addition, the mutagenicity was markedly enhanced by nitroreductase-overproducing mutants such as YG1021 and YG1026, and by *O*-acetyltransferase-overproducing mutants such as YG1024 and YG1029. It was considered that these nitro groups were metabolically reduced to nitroso- and amino-derivatives by these enzymes via a hydroxylamino-intermediate.

Two 1,5- and 1,8-diNAphOs were potent mutagens for TA98 and 100, and showed strong reversion from autotrophy to prototrophy by nitroreductase and *O*-acetyltransferase. Comparing the mutagenic potency of both compounds, 1,8-diNAphO was more strongly activated by nitroreductase than 1,5-diN-4-AphO, e.g. the compound showed 48 850 revertants/μg for YG1026. From the perspective of reduction property, the reduction potentials (mV) of mono- and dinitrophenanthrenes differed; the potentials (Epc1) of mononitrophenanthrenes ranged from −853 to −1214, and those of dinitrophenanthrene (diNph) ranged from −623 to −916 (Table 1). As suggested by Fukuhara et al. [1], nitro substitution causes about a 100–300 mV positive shift in the reduction potentials. Therefore, it was found that the calculated LUMO energy levels were significantly correlated with the first reduction potentials, and the mutagenic potency of NAph was related to these chemical properties, including LUMO energy and reduction potentials.

With regard to mutagenicity and genotoxicity of nitroazabenzo[*a*]pyrene, we reported that these compounds were potent mutagens for *Salmonella* strains [18], and induced micronuclei in polychromatic erythrocytes in mice and chromosomal aberrations in Chinese hamster lung fibroblast cells [19]. Mutagenicity and genotoxicity of nitroazabenzo[*a*]pyrene *N*-oxides differed from substitution of nitro function. However, the reduction potentials of 3-nitro-6-azabenzo[*a*]pyrene *N*-oxide are not markedly different from those of 1-nitro-6-azabenzo[*a*]pyrene *N*-oxide [18]. In addition, 3,6-dinitrobenzo[*a*]pyrene was much more mutagenic than 1,6-dinitrobenzo[*a*]pyrene. This result indicates that 3,6-dinitrobenzo[*a*]pyrene was readily reduced to stronger nitroso- and amino-derivatives than 1,6-dinitrobenzo[*a*]pyrene [20].

As for a human effect of nitrated aromatic compounds, various chemicals deposited in lung tissues were determined after surgical lung resection; e.g. 1-NP, 1,3-DNP and 3-nitrofluoranthene deposited at higher levels in lung tissues decreased the 5-year survival of patients [21]. It was assumed that increasing amounts of mutagens in lung tissues might promote cell differentiation, with an increase in poor differentiation. As reported previously [3], Nph derivatives were detected in diesel emission particulates, but not from other environmental materials and human lung tissues.

Shmeiser et al. [13,22] demonstrated that aristolochic acid containing Nph carboxylic acids induced multiple tumors in the forestomach, ear duct and small intestine, and urothelial cancer in aristolochic acid nephropathy patients [8]. In addition, DNA adducts of the compound were detected in vitro by incubation of calf thymus DNA and liver homogenate, while tumor initiation by aristolochic acid was associated with carcinogen deoxyadenosine adducts as critical lesions.

We therefore, believe that these mutagens are ubiquitous in the environment, though they have not been detected from environmental materials. It is important that the carcinogenicity of these chemicals be studied in more detail to evaluate

the structure activity relationship of NAphs and their danger to human tissues.

References

[1] K. Fukuhara, N. Miyata, Chemical oxidation of nitrated polycyclic aromatic hydrocarbons: Hydroxylation with superoxide anion radical, Chem. Res. Toxicol. 8 (1995) 27–33.

[2] K. Fukuhara, M. Takei, H. Kageyama, N. Miyata, Di- and trinitrophenanthrenes: synthesis, separation, and reduction property, Chem. Res. Toxicol. 8 (1995) 47–54.

[3] N. Sera, K. Fukuhara, N. Miyata, H. Tokiwa, Mutagenicity of nitrophenanthrene derivatives for *Salmonella typhimurium*: effects of nitroreductase and acetyltransferase, Mutat. Res. 349 (1995) 137–144.

[4] P.P. Fu, Yi.-C. Ni, Y.-M. Zhang, R.H. Heflich, Y.-K. Wang, J.-S. Lai, Effect of the orientation of nitro substituent on the bacterial mutagenicity of nitrobenzo[*e*]pyrenes, Mutat. Res. 225 (1989) 121–125.

[5] T. Hirayama, T. Watanabe, M. Akita, S. Shimomura, Y. Fujioka, S. Ozasa, S. Fukui, Relationships between structure of nitrated arenes and their mutagenicity in *Salmonella typhimurium*: 2- and 2,7-nitro substituted fluorene, phenanthrene and pyrene, Mutat. Res. 209 (1988) 67–74.

[6] W.A. Vance, D. Levin, Structural features of nitroaromatics that determine mutagenic activity in *Salmonella typhimurium*, Environ. Mutagen 6 (1984) 797–811.

[7] L. Graeza, P. Ruff, Einfache methods zur bestimmung der aristolochia-sauren durch HPLC, Dtsch. Apoth. Ztg 121 (1981) 2817–2818.

[8] V.M. Arlt, M. Stiborova, H.H. Schmeiser, Aristolochic acid as a probable human cancer hazard in herbal remedies: a review, Mutagenesis 17 (2002) 265–277.

[9] J.M. Pezzuto, S.M. Swanson, W. Mar, C-T. Che, G.A. Cordell, H.H.S. Fong, Evaluation of the mutagenic and cytostatic potential of aristolochic acid (3,4-methylenedioxy-8-methyoxy-10-nitrophenanthrene-1-carboxylic acid) and several of its derivatives, Mutat. Res. 206 (1988) 447–454.

[10] H.H. Schmeiser, B.L. Pool, M. Wiessler, Mutagenicity of the two main components of commercially available carcinogenic aristolochic acid in *Salmonella typhimurium*, Cancer Lett. 23 (1984) 97–101.

[11] U. Mengs, On the histopathogenesis of rat forestomach carcinoma caused by aristolochic acid, Arch. Toxicol. 52 (1983) 209–220.

[12] U. Mengs, W. Lang, J-A. Poch, The Carcinogenic action of aristolochic acid in rats, Arch. Toxicol. 51 (1982) 107–119.

[13] H.H. Schmeiser, J.W.G. Janssen, J. Lyons, H.R. Scherf, W. Pfau, A. Buchmann, C.R. Bartram, M. Wiessler, Aristolochic acid activities *ras* genes in rat tumors at deoxyadenosine residues, Cancer Res. 50 (1990) 5464–5469.

[14] A.K. Debnath, R.L. Lopez de Compadre, A.J. Shusterman, C. Hansch, Quantitative structure–activity relationship investigation of the role of hydrophobicity in regulating mutagenicity in the Ames test: 2. Mutagenicity of aromatic and heteroaromatic nitro compounds in *Salmonella typhimurium* TA100, Environ. Mol. Mutagen 19 (1992) 53–70.

[15] H. Jung, A.U. Shaikh, R.H. Heflich, P.P. Fu, Nitro group orientation, reduction potential, and direct-acting mutagenicity of nitro-polycyclic aromatic hydrocarbons, Environ. Mol. Mutagen. 17 (1991) 169–180.

[16] M.J.S. Dewar, E.W.T. Warford, Electrophile substitution Part III. The nitration of phenanthrene, J.Am.Chem.Soc. (1956) 3570–3572.

[17] M. Watanabe, M. Ishiodate, T. Nohmi, Sensitive method for the detection of mutagenic nitroarenes and aromatic amines: new derivatives of *Salmonella typhimurium* tester strains possessing elevated *O*-acetyltransferase levels, Mutat. Res. 234 (1990) 337–348.

[18] N. Sera, K. Fukuhara, N. Miyata, K. Horikawa, H. Tokiwa, Mutagenicity of nitroazabenzo[*a*]pyrene and its related compounds, Mutat. Res. 280 (1992) 81–85.

[19] N. Sera, K. Fukuhara, N. Miyata, H. Tokiwa, Micronucleus induction and chromosomal aberration of 1- and 3-nitroazabenzo[*a*]pyrene and their *N*-oxides, Mutagenesis 16 (2001) 183–187.

[20] H. Tokiwa, N. Sera, A. Nakashima, K. Nakashima, Y Nakanishi, N. Shigematu, Mutagenic and carcinogenic significance and the possible induction of lung cancer by nitro aromatic hydrocarbons in particulate pollutants, Environ. Health Pers. 102 (1992) 107–110.

[21] H. Tokiwa, N. Sera, Contribution of nitrated polycyclic aromatic hydrocarbons in diesel particles to human lung cancer induction, Polycyclic Aromatic Compounds 21 (2000) 231–245.

[22] H.H. Schmeiser, K.B. Schoepe, M. Wiessler, DNA adduct formation of aristolochic acid I and II in vitro and in vivo, Carcinogenesis 9 (1987) 297–303.

Activation of the Human Ah Receptor by Aza-Polycyclic Aromatic Hydrocarbons and Their Halogenated Derivatives

Ken-ichi SAEKI,*[a] Tomonari MATSUDA,[b] Taka-aki KATO,[a] Katsuya YAMADA,[a] Takaharu MIZUTANI,[a] Saburo MATSUI,[b] Kiyoshi FUKUHARA,[c] and Naoki MIYATA[a,c]

[a] *Faculty of Graduate School of Pharmaceutical Sciences, Nagoya City University: Tanabedori, Mizuho-ku, Nagoya 467–8603, Japan:* [b] *Department of Environmental Engineering, Kyoto University: Sakyo-ku, Yoshida-honmachi, Kyoto 606–8501, Japan: and* [c] *Division of Organic Chemistry, National Institute of Health Sciences: 1–18–1 Kamiyoga, Setagaya-ku, Tokyo 158–8501, Japan.*

Received October 25, 2002; accepted January 31, 2003; published online February 6, 2003

Aryl hydrocarbon receptor (AhR) is a ligand-activated transcription factor through which dioxins and carcinogenic polycyclic aromatic hydrocarbons cause altered gene expression and toxicity. Ten aza-polycyclic aromatic hydrocarbons (aza-PAHs), consisting of nitrogen substituted naphthalenes, phenanthrenes, chrysenes, and benzo[*a*]pyrenes (BaPs), were subjected to analysis of their structure-activity relationships as an AhR ligand by using a yeast AhR signaling assay, in which AhR ligand activity was evaluated as *lacZ* units. Most of the aza-PAHs showed similar or more potent AhR ligand activities than the corresponding parent PAHs. About a 100-fold increased in ligand activity was observed in 10-azaBaP compared with BaP. Halogen-substitution effects on AhR ligand activity in aza-polycyclic aromatics were also investigated with quinoline, benzo[*f*]quinoline (BfQ), benzo[*h*]quinoline (BhQ) and 1,7-phenanthroline (1,7-Phe). Position-specific induction of AhR ligand activity was observed in aza-tricyclic aromatic compounds, BfQ, BhQ, and 1,7-Phe, and the ratio of the ligand activities (*lacZ* units/μM) of monochlorinated and monobrominated aza-tricyclic aromatic compounds to those of the corresponding parent non-halogenated compounds ranged from 2.2- to 254-fold. Greatest enhancement of ligand activity was observed in 2-brominated BfQ (2-Br-BfQ), and its ligand activity was higher than that of BaP. These results suggest that even monohalogenation markedly enhances AhR ligand activity in aza-PAHs.

Key words aryl hydrocarbon receptor; aza-polycyclic aromatic compound; halogenated derivative; structure-activity relationship

Aryl hydrocarbon receptor (AhR) is a ligand-activated transcription factor that mediates cellular responses to numerous environmental contaminants, such as 2,3,7,8-tetrachlorodibenzo-*p*-dioxin (TCDD) and polycyclic aromatic hydrocarbons (PAHs).[1–3] Benzo[*a*]pyrene (BaP) and chrysene are carcinogenic PAHs present in air pollutants from the industrial furnace gas and cigarette smoke.[6] *N*-Containing PAHs, such as azaBaPs, benzoquinolines, phenanthrolines, and quinolines, are also found in air pollutants.[5,7] Although many *N*-containing PAHs exist in environmental pollutants, there has been no data for their AhR ligand activity. We investigated structure-AhR ligand activity relationships of AhR ligand among *N*-containing and non-*N*-containing PAHs using ten nitrogen-substituted naphthalenes, phenanthrenes, chrysenes, and BaPs. In this study, AhR ligand activity was measured by using the yeast AhR signaling assay established by Miller.[8–11] In this screening assay system, the genes of the human AhR and its heterodimer partner, AhR nuclear translocator (Arnt), are co-expressed, and AhR ligand activity can be detected and quantified by measuring the β-galactosidase activity resulting by AhR-mediated transcriptional activation of a *lacZ* reporter plasmid as previously reported.[11] Numerous studies of the effects of halogen-substitution on the AhR ligand activity have been reported.[12] However most of these reports are on dibenzodioxin, dibenzofuran and biphenyl, and there have been few reports on other aromatic nuclei. Therefore, in order to clarify halogen-substitution effects on AhR ligand activity in *N*-containing PAHs, halogen-substituted derivatives of quinoline, benzo[*f*]quinoline (BfQ), benzo[*h*]quinoline (BhQ) and 1,7-phenanthroline (1,7-Phe) were also subjected to the analysis of their structure-AhR ligand activity relationships using the yeast AhR signaling assay system.

MATERIALS AND METHODS

Materials Naphthalene, chrysene, BaP, quinoline, isoquinoline, 1,7-phenanthroline, 1,10-phenanthroline, 4,7-phenanthroline, 2-chloroquinoline (2-Cl-Q), 4-Cl-Q, and 8-bromoquinoline (8-Br-Q) were purchased from Aldrich. Phenanthrene, BfQ, BhQ, 6-Cl-Q, 8-Cl-Q, 3-Br-Q, and 6-Br-Q were purchased from Tokyo Kasei Kogyo Co., Ltd. (Tokyo). 10-Azabenzo[*a*]pyrene (10-azaBaP), 6-azaBaP, 1,10-diazachrysene (1,10-DAC), and 4,10-DAC were synthesized according to the reported methods.[13,14] Most of the fluoroquinolines (F-Qs), consisting of 3-, 5-, 6-, 7-, 8-, 3,5-di, 3,7-di, 5,6-di, 5,7-di, 5,8-di, 6,7-di, 6,8-di, 7,8-di, 3,5,7-tri, 5,6,8-tri, 6,7,8-tri, and 5,6,7,8-tertaF-Q, and fluorinated BhQs (3-, 5-, 6-, 7-, 9-, and 10-F-BhQ), fluorinated BfQs (2- and 7-F-BfQ), and fluorinated 1,7-phenanthlorines (6- and 9-F-1,7-Phe), were synthesized in our laboratory as previously reported.[16,17] 2-Cl-BhQ, 4-Cl-BhQ, 6-Cl-BhQ, 6-Br-BhQ, 2-Br-BfQ, and 9-Cl-1,7-Phe were synthesized as previously reported.[18] 2-F-Q and 2-F-BhQ were synthesized from corresponding chlorinated derivatives, 2-Cl-Q and 2-Cl-BhQ, by the halogen exchange same method as for the synthesis of 2-fluoro-4-methylquinoline from 2-chloro-4-mehtylquinoline described in our report.[19] 3-, 5-, and 7-Cl-Q were synthesized in our laboratory as previously reported.[20] Dichlorinated quinolines (diCl-Qs; 5,8-, 6,8-, and 7,8-diCl-Q), trichlorinated quinolines (triCl-Qs; 5,6,8- and 6,7,8-triCl-Q), and dibrominated quinolines (diBr-Qs; 5,8- and 6,8-diBr-Q)

* To whom correspondence should be addressed. e-mail: saeki@pharm.nagoya-cu.ac.jp

were synthesized from corresponding chlorinated or brominated anilines by the same Skraup reaction method as for the synthesis of 5,7-diCl-Q from 3,5-dichloroaniline described in the literature.[21]

Melting points were determined with a Yamato MP-500D micro-melting point apparatus without correction. Mass spectra were measured with a JEOL JMS-SX102A spectrometer. ^{1}H- and ^{13}C-NMR spectra were recorded with a JEOL JNM-lambda500 spectrometer in $CDCl_3$ using tetramethylsilane as an internal standard. The following compounds were newly synthesized in this study.

2-Chlorobenzo[*f*]quinoline (2-Cl-BfQ): 2-Aminobenzo[*f*]-quinoline[22] (114 mg) was dissolved in conc. HCl (10 ml), and to this solution was added $NaNO_2$ (49 mg, 1.2 eq) at 5 °C. The resulting solution was added to CuCl (67 mg) in 15 ml of conc. HCl at 100 °C, and was kept stirring for 1.5 h at 100 °C. The reaction mixture was poured into water, neutralized with aq. NH_3, extracted with $CHCl_3$, and evaporated. Purification of the extract by column chromatography (silica gel, $CHCl_3$) and recrystallization from MeOH yielded 2-Cl-BfQ as white needles. Yield: 62 mg (56%). mp 96—98 °C. ^{1}H-NMR (500 MHz, $CDCl_3$) δ: 7.68—7.75 (m, 2H, H-8, H-9), 7.95—8.01 (m, 3H, H-5, H-6, H-7), 8.56 (d, J=7.6 Hz, 1H, H-10), 8.89 (d, J=2.2 Hz, 1H, H-3), 8.92 (d, J=2.2 Hz, 1H, H-1). ^{13}C-NMR (125 MHz, $CDCl_3$) δ: 122.75 (C-10), 126.07 (s), 127.41 (C-8 or C-9), 127.62 (C-6), 127.97 (C-8 or C-9), 128.72 (s), 128.82 (C-7), 129.26 (s), 129.73 (C-1), 131.11 (C-5), 131.99 (s), 146.23 (s), 148.66 (C-3). HR-MS *m/z*: 213.0350, Calcd for $C_{13}H_8ClN$: 213.0345.

5-Chloro-1,7-phenanthroline (5-Cl-1,7-Phe): 3,5-Diaminochlorobenzene (1.0 g, 6.7 mmol), glycerol (0.4 ml, 3 eq) and sodium *m*-nitrobenzenesulfonate (0.42 g, 1 eq) were dissolved in 80% H_2SO_4 (20 ml), and the mixture was stirred at 140 °C for 24 h. The reaction mixture was poured into ice water (100 ml). The filtrate was neutralized with aq. NH_3 and extracted with $CHCl_3$. The $CHCl_3$ layer was dried over anhydrous $MgSO_4$ and evaporated. Purification of the extract by column chromatography (aluminum oxide, benzene) and recrystallization from hexane yielded 5-Cl-1,7-Phe as white needles. Yield: 953 mg (67%). mp 118—119 °C. ^{1}H-NMR (500 MHz, $CDCl_3$) δ: 7.57 (m, J=8.5, 4.3 Hz, 1H, H-3 or H-9), 7.62 (m, J=8.5, 4.3 Hz, 1H, H-3 or H-9), 8.13 (s, 1H, H-6), 8.62 (m, J=8.5, 1.8 Hz, 1H, H-4), 8.96 (m, J=4.3, 1.8 Hz, 1H, H-2 or H-8), 9.00 (m, J=4.3, 1.8 Hz, 1H, H-2 or H-8), 9.44 (m, J=8.5, 1.8 Hz, 1H, H-10). ^{13}C-NMR (125 MHz, $CDCl_3$) δ: 122.21 (C-3 or C-9), 122.91 (C-3 or C-9), 124.71 (s), 126.30 (s), 128.49 (C-6), 132.86 (s), 132.95 (C-10), 133.22 (C-4), 146.17 (s), 148.87 (s), 150.07 (C-2 or C-8), 151.94 (C-2 or C-8). MS *m/z*: 214 (M^+), *Anal.* Calcd for $C_{12}H_7ClN_2$: C, 67.15; H, 3.29; N, 13.05. Found: C, 67.41; H, 3.14; N, 13.02.

Yeast Assay for AhR Ligand Activity The YCM3 strain of yeast[8—10] was grown in a synthetic glucose medium overnight at 30 °C in a shaking incubator. On following day 20 μl from the saturated culture was added to 1 ml of a synthetic medium containing 2% galactose as a carbon source. Ligands dissolved in dimethyl sulfoxide were added to the medium to achieve a final solvent concentration of 0.1%. After 18 h, cell densities were determined by reading the spectrophotometric absorbance of the cultures at 595 nm, and 20 μl of the cell suspension was added to 700 μl of Z-buffer (containing 60 mM Na_2HPO_4, 40 mM NaH_2PO_4, 1 mM $MgCl_2$, 10 mM KCl, 2 mM dithiothreitol and 0.2% sarkosyl). The reaction was started by adding 200 μl of *o*-nitrophenyl-β-D-galactopyranoside (4 mg/ml solution in Z-buffer). The samples were incubated for 60 min at 37 °C. Four hundred microliters of 1 M sodium carbonate solution was added to stop the reaction. Absorbances of the reaction mixture were read in a spectrophotometer at 405 nm. The activity of β-galactosidase (referred to *lacZ* units) was calculated by the following formula: absorbance at 405 nm×1000/(absorbance at 595 nm x ml cell suspension added x min reaction time).

RESULTS

The structures of aza-PAHs examined in this study are shown in Fig. 1. A total of 68 aza-PAHs and their halogenated derivatives were tested for AhR ligand activity by the *lacZ* reporter gene assay using the *Saccharomyces cerevisiae* strain YCM3, in which the human AhR and ARNT genes are co-expressed as previously reported.[8—10]

BaP, an exogenous potent AhR ligand, showed an appreciably increase of *lacZ* units in a dose response manner in this assay system (Fig. 2). To compare the activation potencies of aza-PAHs with that of BaP, the concentration of test compounds producing *lacZ* units equivalent to 50% of the maximal *lacZ* units produced by BaP was calculated from the dose-response curve, and expressed as EC_{BaP50}, according to the previously reported method.[23,24] Furthermore, to evaluate the relative activity of halogenated quinolines, BhQs, BfQs, and 1,7-Phes, the value of *lacZ* units per μM of the test compound was also calculated from the slope of the initial linear portion of each dose response curve because quinoline and BfQ showed unsatisfactory levels of maximal induction of *lacZ* units for calculating of the EC_{BaP50} value.

AhR Ligand Activity of Aza-PAHs The AhR ligand activities of ten aza-PAHs were assessed and compared with those of non-*N*-substituted parent skeletons, naphthalene, phenanthrene, chrysene, and BaP (Fig. 2). The ligand activities of penta- and tetra-cyclic aza-PAHs, azaBaPs and DAC's were much higher than that of tri- and di-cyclic aza-PAHs, benzoquinolines, phenanthrolines, quinoline, and isoquinoline, as well as that BaP and chrysene showed extremely potent ligand activities compared with phenathrene and naphthalene. With regard to the effect of the ring nitrogen atom(s) on the AhR ligand activities of PAHs, most of the aza-PAHs showed similar or more potent activities than the corresponding parent PAHs. Greatest enhancing effect (about 100-fold) on AhR ligand activity was obtained by aza-substitution at position-10 in the BaP molecule.

Halogen-Substitution Effects on AhR Ligand Activity of Quinolines The AhR ligand activities of halogenated quinolines are summarized in Table 1, where the ratio of the number of *lacZ* units per μM for halogenated quinolines to that for quinoline is termed as relative activity. All the halogenated quinolines showed more than 3-fold ligand activity increases compared with quinoline. The halogen-substitution effects on ligand activity decrease in the following order regardless of the substituted position, triCl (438- and 783-fold)>diBr (135- and 209-fold) diCl (58- to 176-fold)>Br (14- to 23-fold) Cl (7- to 35-fold) triF (11- to 25-fold)> diF (6- to 14-fold) F (3- to 16-fold).

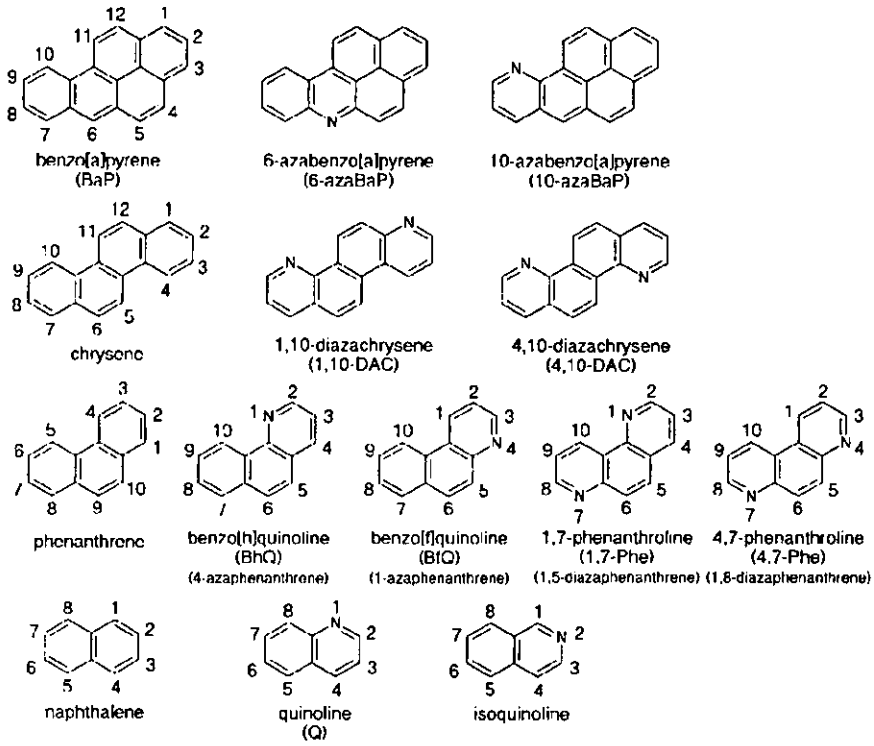

Fig. 1. Structures of PAHs and Aza-PAHs Examined

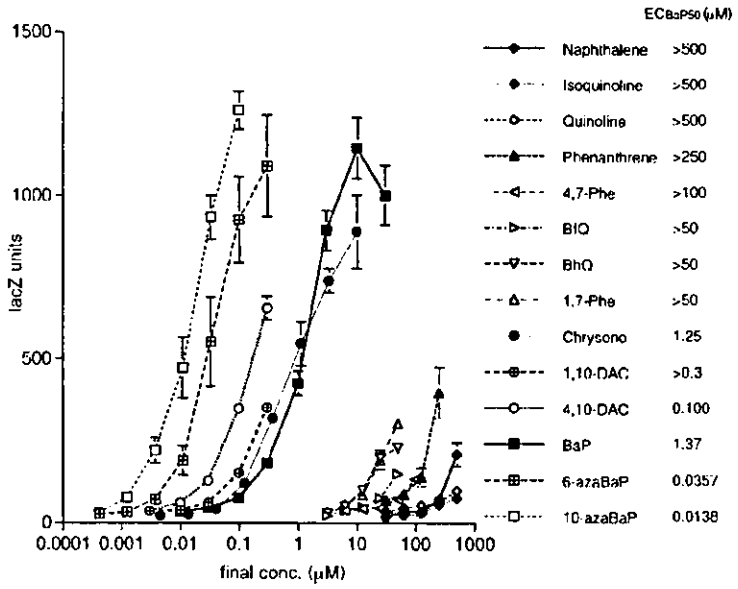

Fig. 2. AhR Ligand Activities of PAHs and Aza-PAHs

AhR ligand activities were assessed by the reporter gene assay using the *Saccharomyces cerevisiae* strain YCM3, in which the human AhR and ARNT genes are co-expressed. Each point represents the mean of at least three analyses. EC_{BaP50} is the concentration producing *lacZ* units equals to 50% of the maximal response to BaP.

Halogen-Substitution Effects on AhR Ligand Activity of Tricyclic Aza-PAHs Monohalogenated analogs of eleven BhQs, four BfQs, and 4 1,7-Phes were assessed and compared with that of each parent compound. The ratio of the number of *lacZ* units per μM for halogenated derivatives to that for the parent compound (relative activity) ranged from 0.3- to 5.8-fold in BhQs, from 6.5- to 254-fold in BfQs, and from 1.7- to 208-fold in 1,7-Phes (Table 2). Cl- and Br-substitution showed greater enhancing effects on AhR ligand activity than F-substitution when compared between the same position analogs, *i.e.*, position-2 and -6 of BhQ, position-2 of BfQ, and position-9 of 1,7-Phe. 2-Cl-BhQ, 2-Br-BfQ, and 9-Cl-1,7-Phe, which are the aza-analogs of 3-halophenanthrene, showed highest AhR ligand activity among the re-

Table 1. AhR Activation Potencies of Q and Its Halogenated Derivatives

Compounds	$EC_{Ba[a]P}$[a] (μM)	*lacZ* units/μM[b]	Relative activity
Quinoline	>500	0.13	1.0
Monofluorinated derivatives			
2-F-Q	>250	0.80	6.2
3-F-Q	>250	1.09	8.4
5-F-Q	250	0.63	4.8
6-F-Q	>250	0.40	3.1
7-F-Q	>250	2.03	15.6
8-F-Q	>250	0.54	4.2
Difluorinated derivatives			
3,5-diF-Q	>250	0.91	7.0
3,7-diF-Q	>250	1.78	13.7
5,6-diF-Q	>250	1.83	14.1
5,7-diF-Q	>250	1.02	7.8
5,8-diF-Q	>250	1.14	8.8
6,7-diF-Q	>250	0.77	5.9
6,8-diF-Q	>250	0.80	6.2
7,8-diF-Q	>250	1.27	9.8
Polyfluorinated derivatives			
3,5,7-triF-Q	>250	1.48	11.4
5,6,8-triF-Q	>250	1.95	15.0
6,7,8-triF-Q	158.6	3.30	25.4
5,6,7,8-tetra-F-Q	164.8	3.15	24.2
Monochlorinated derivatives			
2-Cl-Q	141.1	4.50	34.6
3-Cl-Q	>250	1.57	12.1
4-Cl-Q	>250	0.94	7.2
5-Cl-Q	>250	1.85	14.2
6-Cl-Q	>250	1.21	9.3
7-Cl-Q	>250	1.86	14.3
8-Cl-Q	>250	1.74	13.4
Dichlorinated derivatives			
5,7-diCl-Q	>50	7.68	59.1
5,8-diCl-Q	32.3	15.3	118
6,8-diCl-Q	>50	7.58	58.3
7,8-diCl-Q	28.85	22.9	176
Polychlorinated derivatives			
5,6,8-triCl-Q	14.7	56.9	438
6,7,8-triCl-Q	7.2	101.8	783
Brominated derivatives			
3-Br-Q	174.3	2.98	22.9
6-Br-Q	>250	1.81	13.9
8-Br-Q	172.9	2.71	20.8
Dibrominated derivatives			
5,8-diBr-Q	17.3	27.2	209
6,8-diBr-Q	32.1	17.5	135

Each value is the mean of at least three analyses. *a*) Concentrations producing *lacZ* units equal to 50% of the maximal response to BaP. *b*) Calculated from the slope of the linear portion of each curve near the origin. *c*) Relative values of *lacZ* units/μM of each compound compared to Q.

Table 2. AhR Activation Potencies of BhQs, BfQs, and 1,7-Phes

Compounds	$EC_{Ba[a]P}$[a] (μM)	*lacZ* units/μM[b]	Relative activity
BhQ derivatives			
BhQ	>50	7.47	1.0
2-F-BhQ	29.8	16.7	2.2
3-F-BhQ	>50	8.34	1.1
5-F-BhQ	>50	11.9	1.6
6-F-BhQ	>50	6.80	0.9
7-F-BhQ	>50	11.8	1.6
9-F-BhQ	>50	12.4	1.7
10-F-BhQ	>50	2.53	0.3
3,6-diF-BhQ	>50	5.90	0.8
7,10-diF-BhQ	>50	11.2	1.5
2-Cl-BhQ	13.1	43.3	5.8
4-Cl-BhQ	33.6	22.3	3.0
6-Cl-BhQ	>50	16.3	2.2
6-Br-BhQ	32.2	20.3	2.7
BfQ derivatives			
BfQ	>50	2.62	1.0
2-F-BfQ	26.1	31.6	12.1
7-F-BfQ	30.1	17.0	6.5
7,10-diF-BfQ	16.7	28.2	10.8
2-Cl-BfQ	1.33	247	94.2
2-Br-BfQ	0.65	666	254
1,7-Phenanthroline derivatives			
1,7-Phe	>50	5.91	1.0
6-F-1,7-Phe	>50	9.74	1.6
9-F-1,7-Phe	13.8	43.4	7.3
5-Cl-1,7-Phe	0.44	1117	189
9-Cl-1,7-Phe	0.40	1227	208

Each value is the mean of at least three analyses. *a*) Concentrations producing *lacZ* units equal to 50% of the maximal response to BaP. *b*) Calculated from the slope of the linear portion of each curve near the origin. *c*) Relative values of *lacZ* units/μM of each compound compared to Q.

spective parent compound analogs.

DISCUSSION

We measured the AhR ligand activities of ten *N*-containing PAHs using the yeast AhR signaling assay to investigate the PAH ring nitrogen-substitution effect on the substrate recognition by AhR. Phenanthrene was very weak as the AhR ligand compared with BaP and chrysene, though the ligand activity was altered by nitrogen-substitution in the aromatic ring(s) position-selectively. The ligand activity of phenanthrene was significantly potentiated (about 10-fold) by nitrogen-substitution in position-4 (BhQ) and position-1 and -5 (1,7-Phe), moderately enhanced by nitrogen-substitution in position-1 (BfQ), and not at all affected by nitrogen-substitution in position-1 and -8 (4,7-Phe). BhQ and 1,7-Phe have a nitrogen atom in the bay-region of the molecule, while BfQ and 4,7-Phe do not have one in the bay-region. The result suggests that the N atom in the bay-region is more effective in enhancing the ligand activity than the non-bay-region N atom. Similar enhancing effects by the bay-region N atom(s) were observed in chrysene and BaP. 4,10-DAC, in which two N atoms are located in the bay-region, showed a higher ligand activity than chrysene and 1,10-DAC, in which one N atom is located in the bay-region and the other N atom is located in the non-bay-region. Furthermore, two azaBaPs, 6-azaBaP and 10-azaBaP, showed much higher ligand activities than BaP, and the enhancing effect on ligand activity by *N*-substitution at position-10 (bay-region) was higher than that at position-6 (non-bay-region).

Quinoline, isoquinoline, and naphthalene were about three orders of magnitude less active than BaP. The ligand activity of quinoline was augmented by halogen-substitution 3- to 783-fold. When the enhancing effect of the halogen substituent of quinoline on the AhR ligand activity was compared, chlorine and bromine atoms were more effective than the fluorine atom. Additionally, the enhancing effect on the ligand activity is dependent on the number of the halogen substituents regardless of the substituent position.

A similar result has been reported in polychlorinated naphthalene derivatives, and it is known that the AhR ligand activity of naphthalene is remarkably potentiated by substitu-

tion by more than 3 chlorine atoms.[25,26] It is well known that a majority of potent AhR ligands (*e.g.*, TCDD) are very lipophilic and could fit into a rectangle of 6.8×13.7 Å.[27,28] Quinoline is less lipophilic and smaller in molecular size than TCDD. The enhancement of the AhR ligand activity by oligochlorine- or oligobromine-substitution in quinoline might be explained by the increases of lipophilicity and molecular size.

In *N*-containing tricyclic aromatic hydrocarbons, BhQ and 1,7-Phe showed similar AhR ligand activities and BfQ showed a slightly lower ligand activity than BhQ and 1,7-Phe. However, halogen-substitution effects on the AhR ligand activity in BhQ were much lower than those in BfQ and 1,7-Phe. The AhR ligand activity of BfQ was considerably increased by 2-Cl-substitution (94-fold) and 2-Br-substitution (254-fold) and 5- and 9-Cl-substituion greatly potentiated the ligand activity of 1,7-Phe (189- and 208-fold, respectively), while the effects of Cl- and Br-substitution on the ligand activity of BhQ were only from 2.2- to 5.8-fold potentiation. Furthermore, the ligand activity of BhQ decreased by 66% (to 0.34-fold) by 10-F-substitution. These results suggest that the optimal positionalrelationship for potentiation of the ligand activity exists regarding the position of the nitrogen atom in the aromatic ring and the position of the halogen substituent in *N*-containing tricyclic aromatic hydrocarbons.

With regard to the position specific effect of halogen-substitution on the AhR ligand activity in BhQ, the halogen atom at position-2 was most effective in both cases of fluorine- and chlorine-substitution. Similarly, 2-F-BfQ showed a higher ligand activity than 7-F-BfQ and the ligand activity of 9-F-1,7-Phe was higher than that of 6-F-1,7-Phe. 2-F-BhQ, 2-F-BfQ, and 9-F-1,7-Phe have the common structure of the aza-analog of 3-fluorinated phenanthrene. This finding suggests that the position-3 of phenanthrene is best suited as the site of halogen substitution for potentiation of AhR ligand activity in azaphenanthrenes. In fact, 2-Cl-BfQ, 2-Br-BfQ, and 9-Cl-1,7-Phe showed potent AhR ligand activities (EC_{BaP50} 1.3, 0.7, and 0.4, respectively) equal to or higher than that of BaP (EC_{50} 1.4). This result indicates that the AhR ligand activity of *N*-containing polycyclic aromatics might be markedly enhanced by substitution with only one halogen atom.

In conclusion, the present study on the series of *N*-containing polycyclic aromatics and their halogen-substituted derivatives provides further basic data to better understand the ligand recognition mechanism of AhR and will be useful for prediction of the toxicity of some structurally related environmental pollutants.

Acknowledgments We wish to thank Dr. Charles A. Miller III of Department of Environmental Health Sciences and Tulane-Xavier Center for Bioenvironmental Research, Tulane University School of Public Health and Tropical Medicine, for kindly supplying us with the YCM3 strain. This work was supported in part by Japan Society for the Promotion of Science and the Ministry of Education, Culture, Sports, Science, and Technology of Japan.

REFFERENCES

1) Pohjanvirta R., Tuomisto J., *Pharmacol. Rev.*, **46**, 483–549 (1994).
2) Gonzalez F. J., Fernandez-Salguero P., *Drug Metab. Dispos.*, **12**, 1194–1198 (1998).
3) Okey A. B., Riddick D. S., Harper P. A., *Trends Pharmacol. Sci.*, **15**, 226–232 (1994).
4) Huff J., Lucier G., Tritscher A., *Annu. Rev. Pharmacol. Toxicol.*, **34**, 343–372 (1994).
5) Hankinson O., *Annu. Rev. Pharmacol. Toxicol.*, **35**, 307–340 (1995).
6) Sogawa K., Fujii-Kuriyama Y., *J. Biochem.* (Tokyo), **122**, 1075–1079 (1997).
7) Jerina D. M., Yagi H., Lehr R. E., Thakker D. R., Schaefer-Ridder M., Karle J. M., Levin W., Wood A. W., Chang R. L., Conney A. H., "Polycyclic Hydrocarbons Cancer," Vol. 1, ed. by Gelbin H. V., Ts'o Paul O. P., Academic press, New York, 1978, pp. 173–188.
8) Miller C. A. III, *J. Biol. Chem.*, **272**, 32824–32829 (1997).
9) Miller C. A. III, Martin M. A., Hyman L. E., *Nucleic Acids Res.*, **26**, 3577–3583 (1998).
10) Miller C. A. III, *Tox. Appl. Pharmacol.*, **160**, 297–303 (1999).
11) Adachi J., Mori Y., Matsui S., Takigami H., Fujino J., Kitagawa H., Miller C. A. III, Kato T., Saeki K., Matsuda Y., *J. Biol. Chem.*, **276**, 31475–31478 (2001).
12) Safe S. H., *Ann. Rev. Pharmacol. Toxicol.*, **26**, 371–399 (1986).
13) Karpukins P. P., Slachinskaya A. I., *Vestn. Khar'k. Politekh. Inst.*, **92**, 28–31 (1974).
14) Fukuhara K., Miyata N., *Bull. Natl. Inst. Health Sci.*, **115**, 72–85 (1997).
15) Nekrasov S. V., El'tsov A. V., *Zh. Org. Khim.*, **7**, 188–199 (1971).
16) Saeki K., Kawai H., Kawazoe Y., Hakura A., *Biol. Pharm. Bull.*, **20**, 646–650 (1997).
17) Kato T., Saeki K., Kawazoe Y., Hakura A., *Mutat. Res.*, **439**, 149–157 (1999).
18) Shibata Y., Takeuchi I., Hamada Y., *Yakugaku Zasshi*, **108**, 1148–1153 (1988).
19) Kato T., Hakura A., Mizutani T., Saeki K., *Mutat. Res.*, **465**, 173–182 (2000).
20) Takahashi K., Kamiya M., Sengoku Y., Kawazoe Y., *Chem. Pharm. Bull.*, **36**, 4630–4633 (1988).
21) Palmer M. H., *J. Chem. Soc.*, **1962**, 3645–3652 (1962).
22) Takeuchi I., Hamada Y., Hirota M., *Chem. Pharm. Bull.*, **41**, 747–751 (1993).
23) Kennedy S. W., Lorenzen A., Jones S. P., Hahn M. E., Stegeman J. J., *Toxicol. Appl. Pharmacol.*, **141**, 214–230 (1996).
24) Jones J. M., Anderson J. W., *Environ. Toxicol. Pharmacol.*, **7**, 19–26 (1999).
25) Villeneuve D. L., Khim J. S., Kannan K., Giesy J. P., *Aquatic Toxicol.*, **54**, 125–141 (2001).
26) Ikeda M., Takatsuki M., Yakabe Arimoto Y., Fukuma T., Higashikawa K., *Int. Arch. Occup. Environ. Health*, **74**, 295–301 (2001).
27) Giller M., Bergman J., Cambillau C., Fernström B., Gustafssoon J.-Å., *Mol. Pharmacol.*, **28**, 357–363 (1985).
28) Gillner M., Bergman J., Cambillau C., Alexandersson M., Fernstorom B., Gustafsson J.-Å., *Mol. Pharmacol.*, **44**, 336–345 (1993).

OBC
www.rsc.org/obc

Efficient radical scavenging ability of artepillin C, a major component of Brazilian propolis, and the mechanism

Ikuo Nakanishi,*[a,b] Yoshihiro Uto,[c] Kei Ohkubo,[b] Kentaro Miyazaki,[d,e] Haruko Yakumaru,[a] Shiro Urano,[c] Haruhiro Okuda,[d] Jun-Ichi Ueda,[a] Toshihiko Ozawa,[a] Kiyoshi Fukuhara,[d] Shunichi Fukuzumi,*[b] Hideko Nagasawa,[c] Hitoshi Hori[c] and Nobuo Ikota*[a]

[a] *Redox Regulation Research Group, Research Center for Radiation Safety, National Institute of Radiological Sciences, Inage-ku, Chiba 263-8555, Japan. E-mail: nakanis@nirs.go.jp; Fax: +81-43-255-6819; Tel: +81-43-206-3131*

[b] *Department of Material and Life Science, Graduate School of Engineering, Osaka University, CREST, Japan Science and Technology Corporation, Suita, Osaka 565-0871, Japan. E-mail: fukuzumi@chem.eng.osaka-u.ac.jp; Fax: +81-6-6879-7370; Tel: +81-6-6879-7368*

[c] *Department of Biological Science & Technology, Faculty of Engineering, The University of Tokushima, 2-1 Minamijosanjima-cho, Tokushima 770-8506, Japan*

[d] *Division of Organic Chemistry, National Institute of Health Sciences, Setagaya-ku, Tokyo 158-8501, Japan*

[e] *Department of Applied Chemistry, Shibaura Institute of Technology, Minato-ku, Tokyo 108-8548, Japan*

Received 25th February 2003, Accepted 20th March 2003
First published as an Advance Article on the web 3rd April 2003

Hydrogen transfer from artepillin C to cumylperoxyl radical proceeds *via* one-step hydrogen atom transfer rather than *via* electron transfer, the rate constant of which is comparable to that of (+)-catechin, indicating that artepillin C can act as an efficient antioxidant.

Artepillin C [3-{4-hydroxy-3,5-bis(3-methyl-2-butenyl)phenyl}-2(*E*)-propenoic acid] (**1**), a major component (> 5%) of Brazilian propolis,[1] is a member of a class of 2,4,6-trisubstituted phenols that has recently been reported to show important biological activities, such as antitumor,[2] apoptosis-inducing,[3] immunomodulating,[4] and antioxidative activities.[5] It is known that hydrogen transfer from the phenolic hydroxyl group to active radical species, such as hydroxyl radical ($^{\bullet}OH$), superoxide anion ($O_2^{\bullet-}$), lipid peroxyl radical ($LOO^{\bullet}$), is responsible for the antioxidative activities of the phenolic compounds. However, little is known about the quantitative radical-scavenging ability of **1**, as well as the mechanism of hydrogen-transfer reactions from **1** to radical species. There are two possibilities in the mechanism of hydrogen-transfer reactions from phenolic compounds to radical species, *i.e.*, a one-step hydrogen atom transfer or electron transfer followed by proton transfer.[6] Recently, we have reported that the hydrogen transfer from (+)-catechin, one of the most powerful natural antioxidants, to cumylperoxyl radical proceeds *via* an electron transfer from (+)-catechin to cumylperoxyl radical, which is accelerated by the presence of scandium ion (Sc^{3+}), followed by proton transfer in an aprotic medium.[7] We herein report rates of hydrogen transfer from **1** to cumylperoxyl radical determined by the EPR technique in propionitrile (EtCN) at low temperature (203 K). Cumylperoxyl radical, which is much less reactive than alkoxyl radicals, is known to follow the same pattern of relative reactivity with a variety of substrates.[8–10] The effect of Sc^{3+} on the hydrogen transfer rates was also examined to distinguish between one-step hydrogen- or electron-transfer mechanisms for the radical-scavenging reactions of **1**.

Direct measurements of the rate of hydrogen transfer from **1**† to cumylperoxyl radical were performed in EtCN at 203 K by means of EPR. The photoirradiation of an oxygen-saturated EtCN solution containing di-*tert*-butyl peroxide ($^tBuOO^tBu$) and cumene ($PhCHMe_2$) with a 1000 W high-pressure mercury lamp results in formation of cumylperoxyl radical ($PhC^{\bullet}Me_2OO^{\bullet}$), which was readily detected by EPR. The cumylperoxyl radical is formed *via* a radical chain process shown in eqns. (1)–(3).[11–15] The photoirradiation of $^tBuOO^tBu$ results in the homolytic cleavage of the O–O bond to produce $^tBuO^{\bullet}$ [eqn. (1)],[16,17] which abstracts a hydrogen from cumene to give cumyl radical ($PhC^{\bullet}Me_2$) [eqn. (2)], followed by the facile addition of oxygen to cumyl radical [eqn. (3)]. The cumylperoxyl radical can also abstract a hydrogen atom from cumene in the propagation step to yield cumene hydroperoxide ($PhCMe_2OOH$), accompanied by regeneration of cumyl radical [eqn. (4)].[18,19] In the termination step, cumylperoxyl radicals decay by a bimolecular reaction to yield the corresponding peroxide and oxygen [eqn. (5)].[18,19] When the light is cut off, the EPR signal intensity decays, obeying second-order kinetics due to the bimolecular reaction in eqn. (5). In the presence of **1**, the decay rate of cumylperoxyl radical after cutting off the light becomes much faster than that in the absence of **1**. The decay rate in the presence of **1** ($2.8–5.6 \times 10^{-4}$ M) obeys pseudo-first-order kinetics. This decay process is ascribed to the hydrogen transfer from **1** to cumylperoxyl radical to produce the phenoxyl radical **1**$^{\bullet}$‡ and $PhCMe_2OOH$ [eqn. (6)]. The pseudo-first-order rate constants (k_{obs}) increase with increasing **1** concentration to exhibit first-order dependence on [**1**]. From the slope of the linear plot of k_{obs} *vs.* the concentration of **1** is determined the second-order rate constant (k_{HT}) for the hydrogen transfer from **1** to cumylperoxyl radical as 4.9×10^2 M^{-1} s^{-1} in EtCN at 203 K. This value is very close to the rate constant obtained for hydrogen transfer from (+)-catechin to cumylperoxyl radical in EtCN (6.0×10^2 M^{-1} s^{-1}),[7] indicating that, in aprotic medium, artepillin C is an excellent free radical scavenger, comparable to (+)-catechin.

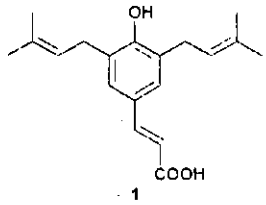

1

DOI: 10.1039/b302098c

$$^tBuOO^tBu \xrightarrow{h\nu} 2\,^tBuO^{\bullet} \quad (1)$$

$$PhCHMe_2 + {}^tBuO^{\bullet} \rightarrow PhC^{\bullet}Me_2 + {}^tBuOH \quad (2)$$

$$PhC^{\bullet}Me_2 + O_2 \rightarrow PhCMe_2OO^{\bullet} \quad (3)$$

$$PhCMe_2OO^{\bullet} + PhCHMe_2 \rightarrow PhCMe_2OOH + PhC^{\bullet}Me_2 \quad (4)$$

$$2\,PhCMe_2OO^{\bullet} \rightarrow (PhCMe_2O)_2 + O_2 \quad (5)$$

1 + $PhCMe_2OO^{\bullet}$ $\xrightarrow{k_{HT}}$ **1**$^{\bullet}$ + $PhCMe_2OOH$ (6)

If the hydrogen transfer from **1** to cumylperoxyl radical involves an electron-transfer process as the rate-determining step, the rate of hydrogen transfer would be accelerated by the presence of scandium ion.[7,20] This is checked by examining the effect of $Sc(OTf)_3$ (OTf = OSO_2CF_3) on the hydrogen-transfer rate from **1** to cumylperoxyl radical. No effect of Sc^{3+} on the k_{HT} values of the hydrogen-transfer reaction of **1** with cumylperoxyl radical used as a hydrogen abstracting agent was observed, as shown in Fig. 1. Thus, there may be no contribution of electron transfer from **1** to cumylperoxyl radical in the hydrogen-transfer reaction, which may thereby proceed *via* a one-step hydrogen atom-transfer process. On the other hand, the hydrogen transfer from (+)-catechin (**2**) to cumylperoxyl radical has been reported to proceed *via* electron transfer from **2** to cumylperoxyl radical, which is accelerated by the presence of Sc^{3+}, followed by proton transfer from the radical cation of **2** to cumylperoxylate (Scheme 1).[7] The difference in the hydrogen-transfer mechanism between **1** and **2** may be ascribed to the oxidation potentials of **1** and **2**. In fact, the oxidation potential of **1** (E^0_{ox} = 1.39 V *vs.* SCE) determined by second-harmonic alternating current voltammetry (SHACV)[21] with a Pt working electrode in acetonitrile, containing 0.1 M n-Bu_4NClO_4 as a supporting electrolyte, is significantly more positive than that of **2** (E^0_{ox} = 1.18 V *vs.* SCE). In such a case, the electron-transfer oxidation of **1** by cumylperoxyl radical, whose

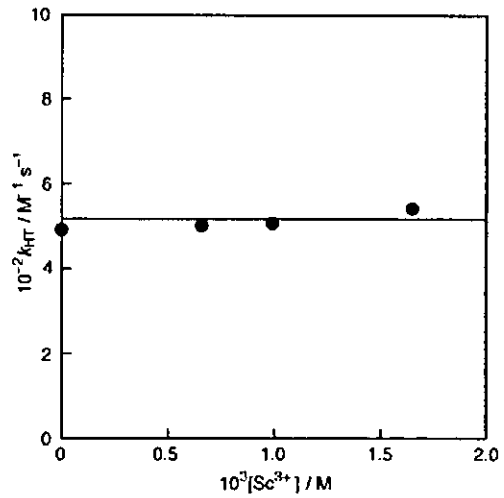

Fig. 1 Plot of k_{HT} *vs.* $[Sc^{3+}]$ in the hydrogen transfer from **1** to cumylperoxyl radical in the presence of $Sc(OTf)_3$ in EtCN at 203 K.

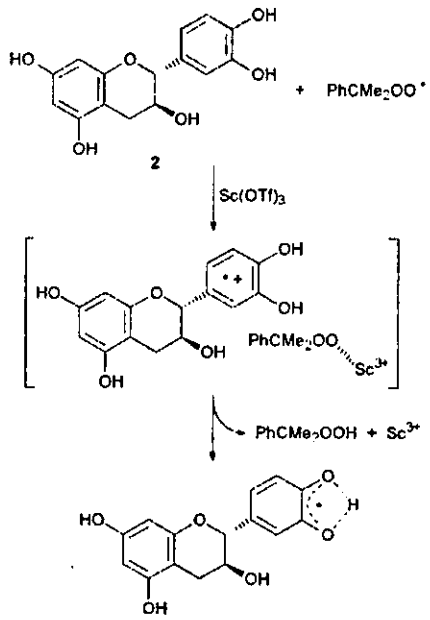

Scheme 1 Mechanism of hydrogen transfer from (+)-catechin (**2**) to cumylperoxyl radical *via* electron transfer.

reduction potential (E^0_{red}) is located at 0.65 V *vs.* SCE,[7] is less energetically feasible than that of **2**.

In conclusion, artepillin C shows an efficient radical-scavenging activity against cumylperoxyl radical in an aprotic medium, which is comparable to that of (+)-catechin. The absence of an effect of Sc^{3+} on the k_{HT} values demonstrates that the hydrogen transfer from artepillin C to cumylperoxyl radical proceeds *via* one-step hydrogen atom transfer rather than *via* an electron transfer followed by proton transfer.

Acknowledgements

This work was partially supported by a Grant-in-Aid for Scientific Research Priority Area (No. 11228205) and a Grant-in-Aid for Young Scientists (B) (No. 13770507) from the Ministry of Education, Culture, Sports, Science and Technology, Japan.

Notes and references

† Synthesis of **1** was carried out according to the procedure reported in the literature. See: Y. Uto, A. Hirata, T. Fujita, S. Takubo, H. Nagasawa and H. Hori, *J. Org. Chem.*, 2002, **67**, 2355.

‡ The EPR signal of phenoxyl radical **1**$^{\bullet}$ has successfully been detected in the photoreaction of **1** with $^tBuOO^tBu$ in CH_2Cl_2, however, no hyperfine structure was observed because of its instability.

1 H. Aga, T. Shibuya, T. Sugimoto, S. Nakajima and M. Kurimoto, *Biosci., Biotechnol., Biochem.*, 1994, **58**, 945.
2 T. Kimoto, S. Arai, M. Aga, T. Hanaya, M. Kohguchi, Y. Nomura and M. Kurimoto, *Gan to Kagaku Ryoho*, 1996, **23**, 1855.
3 T. Matsuno, S. K. Jung, Y. Matsumoto, M. Saito and J. Morikawa, *Anticancer Res.*, 1997, **17**, 3565.
4 T. Kimoto, S. Arai, M. Kohguchi, M. Aga, Y. Nomura, M. J. Micallef, M. Kurimoto and K. Mito, *Cancer Detect. Prev.*, 1998, **22**, 506.
5 K. Hayashi, S. Komura, N. Isaji, N. Ohishi and K. Yagi, *Chem. Pharm. Bull.*, 1999, **47**, 1521.
6 J. S. Wright, E. R. Johnson and G. A. DiLabio, *J. Am. Chem. Soc.*, 2001, **123**, 1173.
7 T. Nakanishi, K. Miyazaki, T. Shimada, K. Ohkubo, S. Urano, N. Ikota, T. Ozawa, S. Fukuzumi and K. Fukuhara, *J. Phys. Chem. A*, 2002, **106**, 11123.
8 G. A. Russel, in *Free Radicals*, ed. J. K. Kochi, Wiley & Sons, New York, 1973, Chapter 7.
9 G. A. Russel, *Can. J. Chem.*, 1956, **34**, 1074.

10 J. A. Howard, K. U. Ingold and M. Symonds, *Can. J. Chem.*, 1968, **46**, 1017.
11 R. A. Sheldon, in *The Activation of Dioxygen and Homogeneous Catalytic Oxidation*, eds. D. H. R. Barton, A. E. Martell and D. T. Sawyer, Plenum, New York and London, 1993, pp. 9–30.
12 G. W. Parshall and S. D. Ittel, in *Homogeneous Catalysis*, Wiley, New York, 2nd edn., 1992, Chapter 10.
13 R. Sheldon and J. K. Kochi, *Adv. Catal.*, 1976, **25**, 72.
14 A. E. Shilov, in *Activation of Saturated Hydrocarbons by Transition Metal Complexes*, D. Reidel Publishing Co., Dordrecht, The Netherlands, 1984, Chapter 4.
15 A. Bottcher, E. R. Birnbaum, M. W. Day, H. B. Gray, M. W. Gristaff and J. A. Labinger, *J. Mol. Catal.*, 1997, **117**, 229.
16 J. K. Kochi, in *Free Radicals in Solution*, J. Wiley & Sons, New York, 1957.
17 (*a*) J. K. Kochi, P. J. Krusic and D. R. Eaton, *J. Am. Chem. Soc.*, 1969, **91**, 1877; (*b*) J. K. Kochi and P. J. Krusic, *J. Am. Chem. Soc.*, 1968, **90**, 7155; (*c*) J. K. Kochi and P. J. Krusic, *J. Am. Chem. Soc.*, 1969, **91**, 3938; (*d*) J. K. Kochi and P. J. Krusic, *J. Am. Chem. Soc.*, 1969, **91**, 3942; (*e*) J. K. Kochi and P. J. Krusic, *J. Am. Chem. Soc.*, 1969, **91**, 3944; (*f*) J. A. Howard and E. Furimsky, *Can. J. Chem.*, 1974, **54**, 555.
18 S. Fukuzumi and Y. Ono, *J. Chem. Soc. Perkin Trans. 2*, 1977, 622.
19 S. Fukuzumi and Y. Ono, *J. Chem. Soc. Perkin Trans. 2*, 1977, 784.
20 S. Fukuzumi and K. Ohkubo, *Chem. Eur. J.*, 2000, **6**, 4532.
21 (*a*) T. G. McCord and D. E. Smith, *Anal. Chem.*, 1969, **41**, 1423; (*b*) A. M. Bond and D. E. Smith, *Anal. Chem.*, 1974, **46**, 1946; (*c*) M. R. Wasielewski and R. Breslow, *J. Am. Chem. Soc.*, 1976, **98**, 4222; (*d*) E. M. Arnett, K. Amarnath, N. G. Harvey and J.-P. Cheng, *J. Am. Chem. Soc.*, 1990, **112**, 344; (*e*) M. Patz, H. Mayr, J. Maruta and S. Fukuzumi, *Angew. Chem., Int. Ed. Engl.*, 1995, **34**, 1225.

ARTICLE

OBC www.rsc.org/obc

Kinetic study of the electron-transfer oxidation of the phenolate anion of a vitamin E model by molecular oxygen generating superoxide anion in an aprotic medium †

Ikuo Nakanishi,*[a,b] Kentaro Miyazaki,[c,d] Tomokazu Shimada,[c,d] Yuko Iizuka,[c] Keiko Inami,[c] Masataka Mochizuki,[c] Shiro Urano,[d] Haruhiro Okuda,[c] Toshihiko Ozawa,[a] Shunichi Fukuzumi,*[b] Nobuo Ikota *[d] and Kiyoshi Fukuhara *[c]

[a] *Redox Regulation Research Group, Research Center for Radiation Safety, National Institute of Radiological Sciences, Inage-ku, Chiba 263-8555, Japan. E-mail: nakanis@nirs.go.jp; Fax: +81-43-255-6819*

[b] *Department of Material and Life Science, Graduate School of Engineering, Osaka University, CREST, Japan Science and Technology Agency, Suita, Osaka 565-0871, Japan. E-mail: fukuzumi@chem.eng.osaka-u.ac.jp; Fax: +81-6-6879-7370*

[c] *Division of Organic Chemistry, National Institute of Health Sciences, Setagaya-ku, Tokyo 158-8501, Japan*

[d] *Department of Applied Chemistry, Shibaura Institute of Technology, Minato-ku, Tokyo 108-8548, Japan*

[e] *Division of Organic and Bioorganic Chemistry, Kyoritsu College of Pharmacy, Mitato-ku, Tokyo 105-8512, Japan*

Received 18th June 2003, Accepted 23rd September 2003
First published as an Advance Article on the web 13th October 2003

Electron-transfer reduction of molecular oxygen (O_2) by the phenolate anion (**1**$^-$) of a vitamin E model, 2,2,5,7,8-pentamethylchroman-6-ol (**III**), occurred to produce superoxide anion, which could be directly detected by a low-temperature EPR measurement. The rate of electron transfer from **1**$^-$ to O_2 was relatively slow, since this process is energetically unfavourable. The one-electron oxidation potential of **1**$^-$ determined by cyclic voltammetric measurements is sufficiently negative to reduce 2,2-bis(4-*tert*-octylphenyl)-1-pierylhydrazyl radical (DOPPH$^\cdot$) to the corresponding one-electron reduced anion, DOPPH$^-$, suggesting that **1**$^-$ can also act as an efficient radical scavenger.

Introduction

Vitamin E (α-tocopherol) is one of the most important biological phenolic antioxidants that can act as an efficient hydrogen-atom donor to active oxygen radicals, such as hydroxyl radical ($^\cdot$OH) and lipid peroxyl radical (LOO$^\cdot$), showing efficient antioxidative activities against oxidative stress in biological systems.[1] In addition to its protective radical-scavenging action, α-tocopherol is known to promote low-density lipoprotein (LDL) oxidation,[2] which is an important event in the development of atherosclerosis.[3] The oxidation of LDL may be catalyzed by metal ions in advanced atherosclerotic lesions[4–6] and α-tocopherol can act as a pro-oxidant *via* reduction of Cu(II) to Cu(I).[7] α-Tocopherol has also been reported to produce superoxide anion ($O_2^{\cdot-}$) in apoptosis-induced cells.[8] The apoptosis has been regarded as responsible for the cell toxicity of α-tocopherol.[9–11] Natural-occurring flavonoids such as (+)-catechin and quercetin are also known to scavenge active oxygen radicals efficiently.[12] However, there is also considerable evidence for the generation of reactive oxygen species (ROS) by such antioxidants under specific reaction conditions, such as in the presence of a base or metal ions.[13] We have recently reported that the dianion species of (+)-catechin and its derivative are generated under strongly basic conditions and act as a strong electron donor, which can reduce molecular oxygen (O_2) to $O_2^{\cdot-}$.[14,15] Yamashita *et al.* have reported that quercetin induces oxidative DNA damage and forms 8-oxo-dG by reacting with Cu(II).[16] With regard to the antioxidant and pro-oxidant properties of α-tocopherol, there have been a number of reports demonstrating the radical-scavenging ability.[17–21] However, whether generation of $O_2^{\cdot-}$ results from the reaction between α-tocopherol itself and O_2 or not has yet to be clarified.

The present work has been performed to clarify this point by determining the rate for the generation of $O_2^{\cdot-}$ in the reaction between the anion species of an α-tocopherol model, 2,2,5,7,8-pentamethylchroman-6-ol (**III**), and O_2 under basic conditions in an aprotic medium. The radical scavenging ability of the α-tocopherol model anion *via* electron transfer reactions is also reported. Detailed spectroscopic and kinetic analyses provide valuable mechanistic insight into the $O_2^{\cdot-}$ formation by α-tocopherol as well as the radical scavenging ability.

Experimental

Materials

2,2,5,7,8-Pentamethylchroman-6-ol (**III**) was purchased from Wako Pure Chemical Ind. Ltd., Japan. Tetra-*n*-butylammonium hydroxide (1.0 M in methanol) was obtained commercially from Aldrich and used as received. Tetra-*n*-butylammonium perchlorate (Bu_4NClO_4) used as a supporting electrolyte for the electrochemical measurements was purchased from Tokyo Chemical Industry Co., Ltd., Japan, recrystallized from ethanol, and dried under vacuum at 313 K. 2,2-Bis(4-*tert*-octylphenyl)-1-pierylhydrazyl radical (DOPPH$^\cdot$) was obtained commercially from Aldrich. Acetonitrile (MeCN; spectral grade) was purchased from Nacalai Tesque, Inc., Japan and used as received.

† Electronic supplementary information (ESI) available: the cyclic voltammogram of **1**$^-$ and the experimental EPR spectrum of **1**$^\cdot$ with the computer simulation spectrum. See http://www.rsc.org/suppdata/ob/b3/b306758k/

DOI: 10.1039/b306758k

Spectral and kinetic measurements

Since the phenolate anion of **III** (**1**$^-$) is readily oxidized by molecular oxygen (O_2), reactions were carried out under strictly deaerated conditions for generation of **1**$^-$. A continuous flow of Ar gas was bubbled through a MeCN solution containing **III** (2.0×10^{-4} M) in a square quartz cuvette (10 mm i.d.) with a glass tube neck for 10 min. The neck of the cuvette was sealed to ensure that air would not leak into the cuvette by using a rubber septum. A microsyringe was used to inject Bu_4NOMe (0–4.0×10^{-4} M), which was also deaerated, into the cuvette to produce **1**$^-$. UV–vis spectral changes associated with this reaction were monitored using an Agilent 8453 photodiode array spectrophotometer. The reaction of **1**$^-$ with O_2 was carried out by adding a stock solution of **1**$^-$ to an MeCN solution of O_2 in the cuvette. The concentrations of O_2 in the solution were adjusted by purging with Ar, air, or O_2 for 10 min prior to the measurements ($[O_2]$ = 0, 2.7×10^{-3}, or 1.3×10^{-2} M), respectively. The oxygen concentration was determined by the photooxidation of 10-methyl-9,10-dihydroacridine with oxygen in the presence of $HClO_4$ in MeCN as reported previously.[22] The rates of electron transfer from **1**$^-$ to O_2 were determined by monitoring the absorbance change at 325 nm due to **1**$^-$. Pseudo-first-order rate constants (k_{obs}) were determined by least-squares curve fitting using a personal computer. The first-order plots of $\ln(A_\infty - A)$ *vs.* time (where A_∞ and A denote the final absorbance and the absorbance at a given reaction time, respectively) were linear for three or more half-lives, with a correlation coefficient of $r > 0.999$.

Cyclic voltammetry

The cyclic voltammetry measurements were performed on an ALS-630A electrochemical analyzer in deaerated MeCN containing 0.10 M Bu_4NClO_4 as a supporting electrolyte. The Pt working electrode (BAS) was polished with BAS polishing alumina suspension and rinsed with acetone before use. The counter electrode was a platinum wire. The measured potentials were recorded with respect to an $Ag/AgNO_3$ (0.01 M) reference electrode. The $E_{1/2}$ values (*vs.* $Ag/AgNO_3$) were converted to those *vs.* SCE by adding 0.29 V.[23] All electrochemical measurements were carried out at 298 K under an atmospheric pressure of Ar.

EPR measurements

To an oxygen-saturated MeCN solution was added the stock MeCN solution of **1**$^-$ (8.3×10^{-4} M) in a quartz EPR tube (4.5 mm i.d.) and the solution was immediately frozen by liquid nitrogen. The EPR spectrum of $O_2^{\bullet-}$ was taken in a frozen MeCN solution at 77 K using a JEOL X-band spectrometer (JES-FA100) under nonsaturating microwave power conditions. The magnitude of modulation was chosen to optimize the resolution and the signal-to-noise (S/N) ratio of the observed spectra. The g values were calibrated precisely with a Mn^{2+} marker which was used as a reference.

The EPR spectrum of **1**$^\bullet$ produced in the reaction between **1**$^-$ (5.0×10^{-4} M) and DOPPH$^\bullet$ (5.0×10^{-5} M) in deaerated MeCN was measured using a LABOTEC LLC-04B EPR sample tube at 298 K. Computer simulation of the EPR spectra was carried out using Calleo ESR Version 1.2 program (Calleo Scientific Publisher) on a personal computer.

Results and discussion

Generation of the phenolate anion of a vitamin E model

When a vitamin E model **III** (2.0×10^{-4} M) was treated with methoxide anion (MeO$^-$) (0–4.0×10^{-4} M) produced in the reaction between tetra-*n*-butylammonium hydroxide (Bu_4NOH) and methanol in deaerated acetonitrile (MeCN), the absorption band at 294 nm due to **III** decreased, accompanied by an increase in the absorption band at 325 nm with clear isosbestic points at 271 and 302 nm as shown in Fig. 1. Such a red-shift of the absorption band is indicative of formation of the phenolate anion.[24] The spectral change is completed by addition of one equivalent of MeO$^-$ as shown in the inset of Fig. 1. This indicates that **III** reacts with MeO$^-$ to produce the phenolate anion **1**$^-$ [eqn (1)]. The resulting **1**$^-$ is stable under anaerobic conditions.

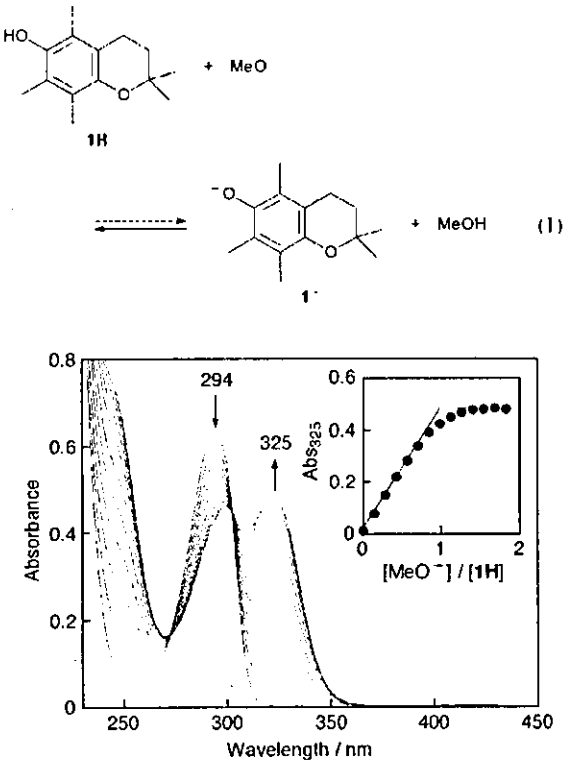

Fig. 1 Spectral change observed upon addition of MeO$^-$ (0–2.0×10^{-4} M) to a deaerated MeCN solution of **III** (2.0×10^{-4} M) at 298 K. Inset: plot of the absorbance at 325 nm (Abs_{325}) *vs.* $[MeO^-]/[\mathbf{III}]$.

Electron-transfer oxidation of the phenolate anion of a vitamin E model by O_2

Introduction of molecular oxygen (O_2) to the MeCN solution of **1**$^-$ resulted in a decrease in the absorption band at 325 nm due to **1**$^-$ as shown in Fig. 2. This spectral change suggests that **1**$^-$ is oxidized by O_2 to produce phenoxyl radical **1**$^\bullet$ and superoxide anion ($O_2^{\bullet-}$) [eqn. (2)]. The formation of $O_2^{\bullet-}$ was confirmed by a low-temperature EPR. A characteristic EPR signal of $O_2^{\bullet-}$ having a $g_{\parallel}$ value of 2.087 was observed for an O_2-saturated MeCN solution of **III** and one equivalent of MeO$^-$ at 77 K as shown in Fig. 3.

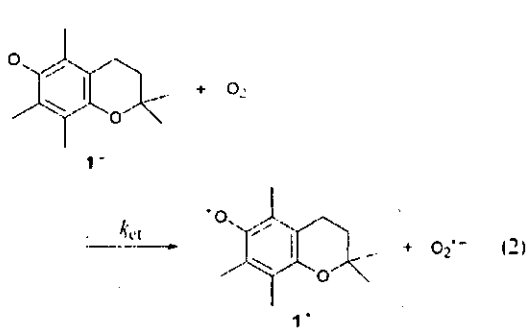

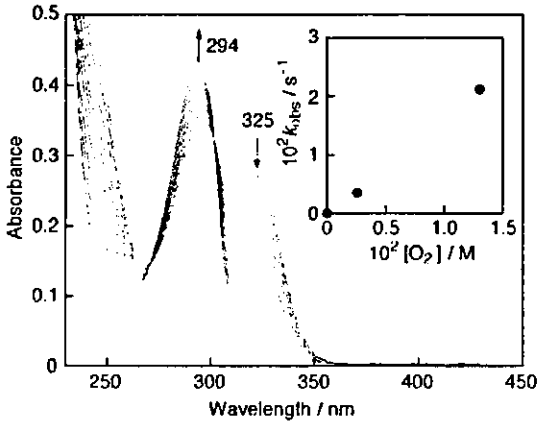

Fig. 2 Spectral change observed in the reaction of **I** (1.0×10^{-4} M) with O_2 (1.3×10^{-2} M) in MeCN at 298 K (30 s intervals). Inset: plot of k_{obs} *vs.* [O_2].

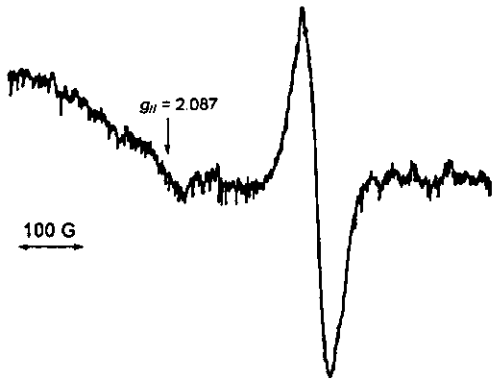

Fig. 3 EPR spectrum of $O_2^{\bullet-}$ generated in the reaction of **I** (8.3×10^{-4} M) with O_2 (1.3×10^{-2} M) in MeCN at 298 K and measured at 77 K.

On the other hand, the EPR signal of **I**$^{\bullet}$ could not be detected in the reaction between **I** and O_2 at 298 K because of the instability of **I**$^{\bullet}$ (*vide infra*). It is known that the phenoxyl radical species derived from *α*-tocopherol and its derivatives decompose *via* a bimolecular disproportionation reaction to produce the parent tocopherols and the corresponding two-electron oxidized products in the absence of O_2.[21,25] In the presence of O_2, radical coupling reactions of phenoxyl radical species of *α*-tocopherol and its derivatives with O_2 are known to occur rapidly to produce a wide variety of oxidized products,[26] which have yet to be identified.

The decrease in the absorbance at 325 nm due to **I** obeyed pseudo-first-order kinetics under conditions where the O_2 concentration (1.3×10^{-2} M)[22] was maintained at more than a 10-fold excess relative to the **I** concentration. The pseudo-first-order rate constant (k_{obs}) increases proportionally with increasing O_2 concentration, as shown in the inset of Fig. 2. The slope of the linear plot of k_{obs} *vs.* [O_2] gave the second-order rate constant of the electron transfer (k_{et}) from **I** to O_2 as 6.7×10^{-1} M^{-1} s^{-1}. The relatively small k_{et} value suggests that the electron transfer from **I** to O_2 is endergonic, where the one-electron oxidation potential of **I** (E^0_{ox}) is more positive than the one-electron reduction potential of O_2 (E^0_{red} *vs.* SCE 0.87 V)[27] (*vide infra*). The rate constant of the disproportionation reaction of **I**$^{\bullet}$ has been determined as 2.7×10^3 M^{-1} s^{-1} in deaerated MeCN at 298 K.[21] This value is much larger than the k_{et} value. In such a case, the electron transfer from **I** to O_2 becomes the rate-determining step, followed by the rapid disproportionation reaction of **I**$^{\bullet}$. Such a follow-up reaction makes it possible to produce $O_2^{\bullet-}$ *via* the endergonic electron transfer. However, the detection of **I**$^{\bullet}$ becomes extremely difficult.

Oxidation potentials of a vitamin E model and its phenolate anion

As mentioned above, the one-electron oxidation potential of **I** (E^0_{ox}) may be more positive than the one-electron reduction potential of O_2 (E^0_{red} *vs.* SCE 0.87 V), leading to the electron transfer from **I** to O_2 an endergonic process [$\Delta G^0_{et} = e(E^0_{ox} - E^0_{red}) > 0$, where ΔG^0_{et} is the free energy change of electron transfer and e is the elementary charge]. Thus, the cyclic voltammetry was performed to determine the one-electron oxidation potential of **I** in deaerated MeCN containing 0.1 M Bu_4NClO_4 as a supporting electrolyte. At a low scan rate (0.10 V s^{-1}), an oxidation peak current of **I** was observed with the smaller reduction peak current in a deaerated MeCN solution containing **III** (2.0×10^{-3} M), MeO (2.0 M), and Bu_4NClO_4 (0.1 M). The smaller reduction peak current of **I**$^{\bullet}$ generated by the electrochemical oxidation as compared to the oxidation peak current of **I** is ascribed to the instability of **I**$^{\bullet}$, which decomposes *via* the bimolecular disproportionation reaction (*vide supra*). At a fast scan rate (2.0 V s^{-1}), the CV becomes reversible (Fig. S1 †). From the midpoint of the redox peaks of the CV of **I** was determined the oxidation potential of **I** (E^0_{ox} *vs.* SCE) as 0.50 V, which is significantly more positive than the E^0_{red} value of O_2 (0.87 V) as expected above. This result is consistent with the relatively small k_{et} value. Since the one-electron oxidation of **III** is known to occur at E^0_{ox} *vs.* SCE 0.77 V, the deprotonation of the phenolic OH group in **III** to form **I** resulted in the very largely negative shift (1.27 V) of the oxidation potential. Thus, the electron transfer reduction of O_2 becomes possible by the deprotonation of **III**. A negative shift of the oxidation potential by deprotonation was also observed between (+)-catechin and its anion species. The oxidation potential of (+)-catechin is E^0_{ox} *vs.* SCE 1.18 V,[28] while that of the anion is located at 0.12 V.[29] In this case, however, no $O_2^{\bullet-}$ is produced by the reaction of the catechin anion with O_2.[30]

Efficient radical-scavenging reaction by the phenolate anion of the vitamin E model

When 2,2-bis(4-*tert*-octylphenyl)-1-picrylhydrazyl radical (DOPPH$^{\bullet}$) is used as an oxidant for **I** instead of O_2, an electron transfer from **I** to DOPPH$^{\bullet}$ occurred very rapidly in deaerated MeCN at 298 K to produce **I**$^{\bullet}$ and DOPPH$^-$ (Scheme 1). This is consistent with the largely negative free energy change of electron transfer from **I** (E^0_{ox} *vs.* SCE 0.47 V) to DOPPH$^{\bullet}$ (E^0_{red} *vs.* SCE 0.18 V). Thus, electron transfer from **I** to DOPPH$^{\bullet}$ is much faster than the bimolecular disproportionation of **I**$^{\bullet}$ and too rapid to be monitored using a stopped-flow technique. In such a case, it becomes possible to detect the resulting **I**$^{\bullet}$ by EPR. The characteristic EPR spectrum having a g value of 2.0047 was observed in the reaction of **I** with DOPPH$^{\bullet}$ (Fig. S2a †) and well reproduced by the computer simulation (Fig. S2b †) using the hyperfine coupling (hfc) values shown in Scheme 1.

Since the one-electron reduction potentials of a variety of peroxyl radicals[31–35] are known to be more positive than the E^0_{red} value of DOPPH$^{\bullet}$, peroxyl radicals may also be scavenged *via* electron transfer from **I** to peroxyl radicals.

In conclusion, the electron-transfer reduction of O_2 by the vitamin E model **III** under basic conditions takes place to produce superoxide anion ($O_2^{\bullet-}$) in MeCN, where the phenolate anion of **III** (**I**$^-$) acts as an actual electron donor to O_2. The one-electron oxidation potential of **I** is sufficiently negative to reduce DOPPH$^{\bullet}$ to DOPPH$^-$. This suggests that the phenolate anion of *α*-tocopherol can also act as an efficient radical scavenger *via* the electron transfer reactions.

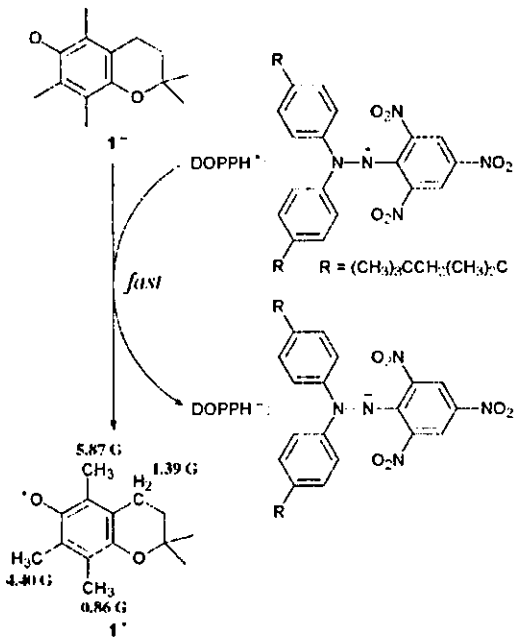

Scheme 1 Reductive DOPPH•-scavenging reaction *via* electron-transfer from **1**• to DOPPH• and the hfc values of the resulting **1**'.

Acknowledgements

This work was partially supported by a Grant-in-Aid for Scientific Research Priority Area (No. 11228205) and a Grant-in-Aid for Young Scientist (B) (No. 15790032) from the Ministry of Education, Culture, Sports, Science and Technology, Japan, partly by a Grant (MF-16) from the Organization for Pharmaceutical Safety and Research, and by a Grant-in-Aid for the Scientific Research (No. 14141201) from the Ministry of Health Labour and Welfare.

References

1 G. W. Burton and K. U. Ingold, *Acc. Chem. Res.*, 1986, **19**, 194.
2 M. J. Burkitt, *Arch. Biochem. Biophys.*, 2001, **394**, 117.
3 D. Steinberg, *J. Biol. Chem.*, 1997, **272**, 20963.
4 C. Smith, M. J. Mitchinson, O. I. Aruoma and B. Halliwell, *Biochem. J.*, 1992, **286**, 901.
5 D. J. Lamb, M. J. Mitchinson and D. S. Leake, *FEBS Lett.*, 1995, **374**, 12.
6 J. Swain and J. M. C. Gutteridge, *FEBS Lett.*, 1995, **368**, 513.
7 Y. Yoshida, E. Niki and N. Noguchi, *Chem. Phys. Lipids*, 2003, **123**, 63.
8 K. Kogure, S. Hama, S. Manabe, A. Tokumura and K. Fukuzawa, *Cancer Lett.*, 2002, **186**, 151.
9 J. M. Turley, T. Fu, F. W. Ruscetti, J. A. Mikovits, D. C. Bertolette and M. C. Birchenall-Roberts, *Cancer Res.*, 1997, **57**, 881.
10 J. Neuzi, I. Svensson, T. Weber, C. Weber and U. T. Brunk, *FEBS Lett.*, 1999, **445**, 295.
11 S. Yamamoto, H. Tamai, R. Ishisaka, T. Kanno, K. Arita, H. Kobuchi and K. Utsumi, *Free Radical Res.*, 2000, **33**, 407.
12 S. V. Jovanovic, S. Steenken, M. Tosic, B. Marjanovic and M. G. Simic, *J. Am. Chem. Soc.*, 1994, **116**, 4846.
13 G. Galati, T. Chan, B. Wu and P. J. O'Brien, *Chem. Res. Toxicol.*, 1999, **12**, 521.
14 I. Nakanishi, K. Fukuhara, K. Ohkubo, T. Shimada, H. Kansui, M. Kurihara, S. Urano, S. Fukuzumi and N. Miyata, *Chem. Lett.*, 2002, 1152.
15 K. Fukuhara, I. Nakanishi, T. Shimada, K. Ohkubo, K. Miyazaki, W. Hakamata, S. Urano, N. Ikota, T. Ozawa, H. Okuda, N. Miyata and S. Fukuzumi, *Chem. Res. Toxicol.*, 2003, **16**, 81.
16 N. Yamashita, H. Tanemura and S. Kawanishi, *Mutat. Res.*, 1999, **425**, 107.
17 U. Svanholm, K. Bachgaard and V. Parker, *J. Am. Chem. Soc.*, 1974, **96**, 2409.
18 G. W. Burton, T. Doba, E. G. Gabe, L. Hughes, F. L. Lee, L. Prasad and K. U. Ingold, *J. Am. Chem. Soc.*, 1985, **107**, 7053.
19 K. Mukai, K. Fukuda, K. Tajima and K. Ishizu, *J. Org. Chem.*, 1988, **53**, 430.
20 K. Mukai, Y. Kageyama, T. Ishida and K. Fukuda, *J. Org. Chem.*, 1989, **54**, 552.
21 I. Nakanishi, K. Fukuhara, T. Shimada, K. Ohkubo, Y. Iizuka, K. Inami, M. Mochizuki, S. Urnao, S. Itoh, N. Miyata and S. Fukuzumi, *J. Chem. Soc., Perkin Trans. 2*, 2002, 1520.
22 S. Fukuzumi, M. Ishikawa and T. Tanaka, *J. Chem. Soc., Perkin Trans. 2*, 1989, 1037.
23 K. Mann and K. K. Barnes, in *Electrochemical Reactions in Nonaqueous Systems*, Marcel Dekker Inc., New York, 1990.
24 S. Itoh, H. Kumei, S. Nagatomo, T. Kitagawa and S. Fukuzumi, *J. Am. Chem. Soc.*, 2001, **123**, 2165.
25 V. W. Bowry and K. U. Ingold, *J. Org. Chem.*, 1995, **60**, 5456.
26 Y. Nagata, C. Miyamoto, Y. Matsushimama and S. Matsumoto, *Chem. Pharm. Bull.*, 1999, **47**, 923
27 D. T. Sawyer and J. L. Roberts, Jr., *Acc. Chem. Res.*, 1988, **21**, 469.
28 I. Nakanishi, Y. Uto, K. Ohkubo, K. Miyazaki, H. Yakumaru, S. Urano, H. Okuda, J.-I. Ueda, T. Ozawa, K. Fukuhara, S. Fukuzumi, H. Nagasawa, H. Hori and N. Ikota, *Org. Biomol. Chem.*, 2003, **1**, 1452.
29 C. Cren-Olive, P. Bapiot, J. Pinson and C. Rolando, *J. Am. Chem. Soc.*, 2002, **124**, 14027.
30 I. Nakanishi, K. Fukuhara, K. Ohkubo, T. Shimada, H. Kansui, M. Kurihara, S. Urano, S. Fukuzumi and N. Miyata, *Chem. Lett.*, 2001, 1152.
31 Z. B. Alfassi, S. Mosseri and P. Neta, *J. Phys. Chem.*, 1989, **93**, 1380.
32 G. I. Khaikin, Z. B. Alfassi and P. Neta, *J. Phys. Chem.*, 1995, **99**, 16722.
33 G. I. Khaikin, Z. B. Alfassi, R. E. Huie and P. Neta, *J. Phys. Chem.*, 1996, **100**, 7072.
34 P. Neta, R. E. Huie and A. B. Ross, *J. Phys. Chem. Ref. Data*, 1990, **19**, 413.
35 M. S. Workentin, F. Maran and D. D. M. Wayner, *J. Am. Chem. Soc.*, 1995, **117**, 2120.

Available online at www.sciencedirect.com
SCIENCE DIRECT®
Chemico-Biological Interactions
Chemico-Biological Interactions 146 (2003) 19–25
www.elsevier.com/locate/chembioint

Structural activity relationship between *Salmonella*-mutagenicity and nitro-orientation of nitroazaphenanthrenes

Hiroshi Tokiwa [a,*], Nobuyuki Sera [b], Kiyoshi Fukuhara [c], Hideo Utsumi [d], Shigeki Sasaki [e], Naoki Miyata [e]

[a] *Department of Environmental Health Science, Kyushu Women's University, 1-1, Jiyugaoka, Yahatanishiku, Kitakyushu, Japan*
[b] *Department of Health Science, Fukuoka Institute of Health and Environmental Sciences, Fukuoka 818-01, Japan*
[c] *National Institute of Health Sciences, Setagaya-ku, Tokyo 158-8501, Japan*
[d] *Laboratory of Bio-function Analysis, Graduate School of Pharmaceutical Sciences, Kyushu University, 3-1-1 Maidashi, Higashi-ku, Fukuoka 812-8582, Japan*
[e] *Bioorganic and Synthetic Chemistry, Graduate School of Pharmaceutical Sciences, Kyushu University, 3-1-1 Maidashi, Higashi-ku, Fukuoka 812-8582, Japan*

Received 12 September 2002; accepted 27 March 2003

Abstract

Nitroazaphenanthrenes (NAphs) and their *N*-oxides (NAphOs) were synthesized as derivatives with nitrogen atoms in the 1, 4, and 9 positions of phenanthrene rings, and as nitrated derivatives substituted at the 1, 2, 3, 4, 5, 6, 7, and 8 positions of phenanthrene rings. To determine the structure activity relationship of these derivatives, all 19 isomers were bioassayed with *Salmonella* tester strains. NAphs substituted at the 4, 6, 7 and 8 positions were mutagenic for TA98, and 1-, 2-, and 3-N-9-AphOs, 6-N-1-AphO and 6-N-4-AphO were mutagenic for TA98 and TA100 without the S9 mix, while 5-N-1-AphO and 5-N-9-AphO were non- or weakly mutagenic. Nitrated derivatives, 6-N-4-Aph, 6-N-9-Aph, 6-N-1-AphO, and 6-N-4-AphO, were powerful mutagens for TA98 and TA100. Mutagenicity was enhanced by mutant strains producing nitroreductase, such as YG1021 and 1026, and by those producing *O*-acetyltransferase, such as YG1024 and 1029. Nitro derivatives substituted at positions 4 and 5 in the phenanthrene rings were perpendicular, while those at positions 2, 3, 6 and 7 were coplanar to the phenanthrene rings. NAphs substituted at the 1 and 8 positions were noncoplanar due to steric hindrance of the aromatic proton at the peri position. On the other hand, 1,5- and 1,8-dinitro-4-azaphenanthrenes showed high mutagenicity for strains TA98 and TA100 in the absence of the S9 mix, and were strongly enhanced by nitroreductase and *O*-acetyltransferase, over-producing mutants. Therefore, it was found that the mutagenic potency of NAphs and NAphOs was closely associated with the chemical properties and orientation of nitro substitution of aromatic rings.

Keywords: Nitroazaphenanthrenes; *Salmonella* mutagenicity; Nitro-orientation

* Corresponding author. Tel.: +81-693-3088; fax: +81-692-3245.
E-mail address: tokiwa@kwuc.ac.jp (H. Tokiwa).

0009-2797/03/$ - see front matter
doi:10.1016/S0009-2797(03)00070-X

1. Introduction

Nitrophenanthrene (Nph) derivatives were synthesized by Fukuhara et al. [1,2], and their mutagenicity was investigated in *Salmonella* strains [3]. It was found that most nitro derivatives showed strong mutagenicity in *Salmonella* mutants, and that the orientation of the nitro substituent had an important structural feature affecting the mutagenic potency and metabolism of Nph [3–5]. Normally, mutagenic activity of nitroarenes is associated with structural features such as the physical dimensions of the aromatic rings, isomeric position of the nitro group, conformation of the nitro group with respect to the plane of the aromatic rings and the ability to resonance-stabilize the ultimate electrophile [6].

Aristolochic acid was used as an anti-inflammatory agent in several pharmaceutical preparations up to 1982, and consisted of several components of Nphs [7]. It was found that Aristolochic acid also contained genotoxic mutagens forming DNA adducts after metabolic activation in *Salmonella* strains and mammalian cells [8–10], as well as being was carcinogenic in rats [11–13]. It has been reported that the mutagenic activity of Nph was closely associated with reduction potentials and the dihedral angles of the nitro substituent for intercalation of chemicals into DNA [2–4,14,15].

Nitroazaphenanthrene (NAph) derivatives containing nitrogen atoms at the 1, 4, and 9 positions of phenanthrene rings were synthesized by Fukuhara et al. (unpublished data), and their reduction property was determined. Using authentic samples of Nph and NAph derivatives, *Salmonella* mutagenicity was determined, and the structural activity relationship was discussed.

2. Materials and methods

2.1. Chemicals

NAphs containing nitrogen atoms in the rings used in this study were 8-nitro-1-azaphenanthrene (8-N-1-Aph), 6- and 8-N-4-APh, 4-, 5-, 6-, and 7-N-9-Aph, 5-, 6- and 8-N-1-Aph *N*-oxide (5-, 6- and 8-N-1-AphO), 5-, 6- and 8-N-4-APhO, 1-, 2-, 3- and 5-N-9-APhO, and 1,5- and 1,8-dinitro-4-APhO (1,5- and 1,8-diN-4-AphO). These NAph derivatives were synthesized by Fukuhara et al. (unpublished data) and modified by the method described by Dewar and Warford [16].

2.2. Bacterial strains

Bacterial strains used were *Salmonella typhimurium* TA98, TA100, and TA98NR, a nitroreductase-deficient mutant of TA98, TA98/1,8DNP, an *O*-acetyltransferase-deficient mutant of TA98, YG1021 and YG1026 produced by transferring a plasmid carrying the nitroreductase gene into cells of TA98 and TA100, respectively, and strains YG1024 and 1029, carrying a plasmid of the acetyltransferase gene transferred into cells of TA98 and TA100, respectively, were generously donated by Drs T. Nohmi and M. Watanabe, National Institute of Health Sciences [17].

2.3. Electrochemical reduction by cyclic voltammetry and electronic descriptors

In dimethylformamide, teraethylammonium perchlorate was used as the supporting electrolyte at a 0.1 M concetration. The reference electrode was an Ag/Ag^+ electrode in acetonitrile with 0.1 M tetrabutylammonium perchlorate. After transfer of the solution containing the test chemical to the cell, it was purged of oxygen by bubbling with N_2 for 15 min. The cyclic voltammograms were recorded at a scan rate of 100 mV/s, while maintaining the test solution under a steady steam of N_2.

The electronic descriptor, LUMO energy levels of nitrated phenanthrenes, was calculated by MOPAC2002 (AM1), which is based on the MOPAC of the Toray System Center using the AM1 method. The initial geometries were constructed from standard bond lengths and angles. The geometries were then completely optimized using algorithms in the MOPAC program. For 5-N-4-AphO and 1,5-diN-4-AphO, LUMO energy and dihedral angle were obtained by AM1 calculations based on the structure that was optimized by PM3.